2006-7035

11th AIAA/ISSMO Multidisciplinary Analysis and Optimization Conference, September 6–8, Portsmouth, Virginia

Strict Constraint Feasibility in Analysis and Design of Uncertain Systems

Luis G. Crespo*

National Institute of Aerospace

Daniel P. Giesy† and Sean P. Kenny†

Dynamic Systems and Control Branch, NASA Langley Research Center.

This paper proposes a methodology for the analysis and design optimization of models subject to parametric uncertainty, where hard inequality constraints are present. Hard constraints are those that must be satisfied for all parameter realizations prescribed by the uncertainty model. Emphasis is given to uncertainty models prescribed by norm-bounded perturbations from a nominal parameter value, i.e., hyper-spheres, and by sets of independently bounded uncertain variables, i.e., hyper-rectangles. These models make it possible to consider sets of parameters having comparable as well as dissimilar levels of uncertainty. Two alternative formulations for hyper-rectangular sets are proposed, one based on a transformation of variables and another based on an infinity norm approach. The suite of tools developed enable us to determine if the satisfaction of hard constraints is feasible by identifying critical combinations of uncertain parameters. Since this practice is performed without sampling or partitioning the parameter space, the resulting assessments of robustness are analytically verifiable. Strategies that enable the comparison of the robustness of competing design alternatives, the approximation of the robust design space, and the systematic search for designs with improved robustness characteristics are also proposed. Since the problem formulation is generic and the solution methods only require standard optimization algorithms for their implementation, the tools developed are applicable to a broad range of problems in

*Staff Scientist, 100 Exploration Way, Hampton VA 23666. AIAA Professional Member.

†Aerospace Technologists, Mail Stop 308, NASA LaRC, Hampton VA, 23681.

several disciplines.

Keywords: optimization, robustness, parametric safety margins.

List of Acronyms

CPV	Critical Parameter Value
CSR	Critical Similitude Ratio
FDS	Feasible Design Space
PSM	Parametric Safety Margin
RDS	Robust Design Space

I. Introduction

Design under uncertainty arises in numerous disciplines including Engineering, Economics, Finance, and Management. Achieving balance between robustness and performance is one of the fundamental challenges faced by scientists and engineers. Trade-offs must be made to reach acceptable levels of performance with adequate robustness to uncertainty.

Literature in probabilistic controls,[1] stochastic programming[2,3] and stochastic approximations[4] provides several mathematical tools for optimization under uncertainty. The algorithms at our disposal can be classified according to the way they enforce inequality constraints that depend on the uncertain parameters. *Hard Constraints*[5–9] are those that, for a given uncertainty model, must be satisfied for all possible realizations of the uncertain parameter (a *realization* is any possible value within the uncertainty model). Strategies to solve the resulting semi-infinite optimization problem usually require nested searches where approximations to the worst-parameter-realization[5,10] are made in a inner optimization loop and a growing number of constraints, which depend on this approximation, are sequentially added to the outer loop. These strategies however, not only become computationally intractable for uncertain parameters of large dimension; but more importantly, are unable to provide guarantees of constraint satisfaction.

For high risk decisions, the achievement and formal verification of strict constraint feasibility are crucial tasks. This paper builds new techniques to address these needs by developing a comprehensive methodology for robustness analysis and robust-design based on the calculation of certain indicators, called Parametric Safety Margins (PSMs), Critical Parameter Values (CPVs), and Critical Similitude Ratios (CSRs). The methodology enables us to determine if strict feasibility is possible. Besides, the tools derived allow for quantifying and comparing the robustness characteristics of competing design alternatives. Those tools are also extended and used for the systematic search of solutions with improved robustness. The ideas proposed do not require sampling/partitioning the parameter space. Instead, they are based on the numerical solution to an optimization problem. Hence, the results are as verifiable as is the convergence to the global optima.

This paper is organized as follows. An informal overview of the paper is given. Then the mathematical formulation is motivated and introduced. Following that, robustness analysis tests for hyper-spherical and hyper-rectangular uncertainty sets are presented. The concepts and tools used for analysis are then extended and applied to robust design. A low-dimensional example is used for illustration. Finally, some concluding remarks are given.

II. Informal Overview

This paper is concerned with questions of analysis and design asked about a system which is described by a parametric mathematical model. The parameters which specify the system are of two sorts – some uncertain parameters which are denoted by the vector $\boldsymbol{p}$ and some design parameters which are denoted by the vector $\boldsymbol{d}$.

The model of uncertainty used in this paper is composed of a support set $\Delta_{\boldsymbol{p}}$ and a designated point $\bar{\boldsymbol{p}} \in \Delta_{\boldsymbol{p}}$ which will be used as an anchor point for defining expansions and contractions of the support set. The value of the uncertain parameter $\boldsymbol{p}$ is not specified but is assumed to belong to the support set $\Delta_{\boldsymbol{p}}$. The choices of $\Delta_{\boldsymbol{p}}$ and $\bar{\boldsymbol{p}}$ are made by some subject matter expert. However, the theory presented in this paper tacitly acknowledges that such a choice may be fairly arbitrary. The problem of when an acceptable design remains acceptable if the uncertainty support set is enlarged (signaling robustness to uncertainty in the original design) is addressed. Conversely, the problem of how much an uncertainty support set must be reduced to make an unacceptable design acceptable (indicating a situation in which it becomes necessary to reduce uncertainty to accomplish design goals) is also addressed.

For analysis purposes, $\boldsymbol{d}$ is assumed to take on a fixed value. For design purposes, $\boldsymbol{d}$ is to be chosen to achieve some design goal(s).

For the purposes of this paper, the salient part of the system model is a finite collection of (real valued) constraint functions which depend on both the uncertain and design parameters. The system is deemed acceptable at given values of the uncertain and design parameters if all constraint functions values are non-positive there. For each value of the design parameter, these functions partition the uncertain parameter space into two regions, a failure region where at least one of the functions takes on a positive value and a region of acceptable uncertain parameter values which comprises everything not in the failure region. The Feasible Design Space is the set of design points (i.e., points in the space of design parameters) for which the constraints are satisfied at the designated point. From this point of view, the designated point is functioning as a nominal value for the uncertain parameter.

One of our tasks is to assign a measure of robustness to a feasible design point based on measuring how much the uncertainty support set can be expanded without encroaching on the failure region. This requires specifying what we mean by expanding the support set. This is where the designated point enters in. Expansion by a factor of α can be viewed in the following way. Imagine standing at the designated point and looking at any other point of the support set. Denote the distance from the designated point to the other point by δ. Then a point will be placed in the expansion set by looking in the same direction, and placing a point at a distance of $\alpha\delta$ from the designated point. Note that if α is less than 1, this actually represents a contraction of the support set. In either case, the geometric terminology is that the new set is *homothetic*[11] to the original. By limiting our attention to hyper-spherical and hyper-rectangular support sets, we are able to cast the problem of finding the maximal feasible expansion of the support set in terms of a problem that standard nonlinear constrained optimization algorithms are applicable to.

The failure domain changes as the design parameter changes. For each different feasible design point, a measure of robustness can be calculated. One can then search for a design which has the greatest measure of robustness. Once again, we show how to cast this search in the form of a nonlinear optimization problem so that existing optimization techniques may be applied.

The first task of this paper is to specify conditions on support set geometry and on the constraint functions so that optimization tools may be applied.

III. Framework

Definition 1 (Uncertainty Model). *The* uncertainty model *of a vector uncertain parameter* $\boldsymbol{p}$ *is the pair* $\langle \Delta_{\boldsymbol{p}}, \bar{\boldsymbol{p}} \rangle$*, where* $\Delta_{\boldsymbol{p}} \subset \mathbb{R}^{\dim(\boldsymbol{p})}$ *is the* support set *and* $\bar{\boldsymbol{p}} \in \Delta_{\boldsymbol{p}}$ *is the* designated point*.*

The uncertainty model is specified by the analyst/designer. The intent is that the set $\Delta_{\boldsymbol{p}}$ be chosen so that the actual value of the uncertain parameter $\boldsymbol{p}$ lies somewhere within it. A *realization* of the uncertain parameter is a value of the parameter selected from $\Delta_{\boldsymbol{p}}$. The designated point, whose selection is subjective, can be interpreted as the realization that best represents $\boldsymbol{p}$, such as a nominal value.

Consider now the situation that a system depends on an uncertain parameter $\boldsymbol{p} \in \mathbb{R}^{\dim(\boldsymbol{p})}$ and a design variable $\boldsymbol{d} \in \mathbb{R}^{\dim(\boldsymbol{d})}$. Suppose that $\boldsymbol{g} : \mathbb{R}^{\dim(\boldsymbol{p})} \times \mathbb{R}^{\dim(\boldsymbol{d})} \rightarrow \mathbb{R}^{\dim(\boldsymbol{g})}$ is a set of constraint functions on the system, which have been normalized so that positive values represent constraint violations. If these are considered hard constraints, the system corresponding to given values of $\boldsymbol{d}$ and $\Delta_{\boldsymbol{p}}$ will be judged acceptable if, $\boldsymbol{g}(\boldsymbol{p}, \boldsymbol{d}) \leq \boldsymbol{0}$, $\forall \boldsymbol{p} \in \Delta_{\boldsymbol{p}}$. The failure region (or infeasible region), denoted as $\mathcal{F}(\boldsymbol{d}, \boldsymbol{g}) \subset \mathbb{R}^{\dim(\boldsymbol{p})}$, is composed of the parameters that do not satisfy all the constraints. For a fixed design $\boldsymbol{d}$, $\mathcal{F}(\boldsymbol{d}, \boldsymbol{g})$ either overlaps the set $\Delta_{\boldsymbol{p}}$, case in which the design $\boldsymbol{d}$ is *non-robust*; or $\mathcal{F}(\boldsymbol{d}, \boldsymbol{g})$ and $\Delta_{\boldsymbol{p}}$ are disjoint, case in which the design $\boldsymbol{d}$ is *robust*. In the latter case, the degree of robustness can be quantified by using the Critical Similitude Ratio (see Definition 4) to measure the separation between the two sets.

Selecting the set $\Delta_{\boldsymbol{p}}$ usually involves some engineering judgment. One reasonable choice might be to confine each component of $\boldsymbol{p}$ to a bounded interval. This leads to the choice of $\Delta_{\boldsymbol{p}}$ as a hyper-rectangle. A natural choice for the designated point $\bar{\boldsymbol{p}}$ is the geometric center of $\Delta_{\boldsymbol{p}}$. If $\boldsymbol{m}$ is the vector of half-lengths of the sides of the hyper-rectangle, the rectangle is represented by the notation $\mathcal{R}_{\boldsymbol{p}}(\bar{\boldsymbol{p}}, \boldsymbol{m})$, and defined by

$$\mathcal{R}_{\boldsymbol{p}}(\bar{\boldsymbol{p}}, \boldsymbol{m}) = \left\{ \boldsymbol{p} : \boldsymbol{p}_i \in [\bar{\boldsymbol{p}}_i - \boldsymbol{m}_i, \bar{\boldsymbol{p}}_i + \boldsymbol{m}_i], 1 \leq i \leq \dim(\boldsymbol{p}) \right\}.$$

Another reasonable choice for $\Delta_{\boldsymbol{p}}$ is a hyper-sphere. The hyper-sphere of radius R centered at $\bar{\boldsymbol{p}}$ will be denoted as $\mathcal{S}_{\boldsymbol{p}}(\bar{\boldsymbol{p}}, R)$.

Definition 2 (Homothetic Sets[11]). *In Euclidean geometry, two sets A and B are called homothetic with respect to the center x at a similitude ratio α if*

$$B = \{b : b = \alpha(a - x) + x, a \in A\}.$$

Such a set B is completely determined by A, x, and α. We use the notation $B = \mathcal{H}(A, x, \alpha)$ to express this relationship.

$B = \mathcal{H}(A, x, \alpha)$ means that B can be created from A by forming every vector from the homothetic center point x to each point of A; stretching or shrinking it by a factor of α; and, with the root-points of the stretched or shrunk vectors all fixed at x, collecting all the new endpoints to form the set B.

For purposes of this paper, two uncertainty models will be called *proportional* if they have the same designated point and they are homothetic with respect to that designated point as homothetic center. This means that one of the two support sets can be formed from the other by expansion or contraction by some positive factor, which is the *similitude ratio* α, about the common designated point. For instance, the hyper-rectangles $\mathcal{R}_{\boldsymbol{p}}(\bar{\boldsymbol{p}}, \boldsymbol{m})$ and $\mathcal{R}_{\boldsymbol{p}}(\bar{\boldsymbol{p}}, \alpha\boldsymbol{m})$ are proportional sets for positive similitude ratios α.

The notions of CPV, PSM, and CSR are now introduced. For the sake of clarity , the presentation of the material will concentrate on the case where the designated point is in the non-failure region. The converse case is considered in Section IV.D. Intuitively, one imagines that a set proportional to the support set of the uncertainty model is being expanded homotheticly with respect to its designated point until its boundary just touches the boundary of the failure region. The point(s) where the expanding set touches the infeasible region is (are) the CPV(s). The CSR is the similitude ratio of that expansion, and the PSM is a metric that quantifies the size of the set proportional to the support set that has the CPV on its surface. Both the CSR, which is defined for all support sets, and the PSM, which is defined for support sets which are hyper-spheres or hyper-rectangles, provide a measure of robustness of a design to parameter uncertainty. The larger they are, the larger the variation from its designated point to which the uncertain parameter can be subjected without encountering a constraint violation. The CSR is non-dimensional, but depends on both the shape and the size of the support set. The PSM has the same units as the uncertain parameters, and depends on the shape, but not the size, of the support set. The geometry of support sets and their homothetic transforms and of constraint violation sets, and particularly the boundaries of these sets, plays a critical role in the results in this paper. The mathematical background for these notions is now presented.

Definition 3 (Constraint Violation Set). *Suppose that $\boldsymbol{g} : \mathbb{R}^{\dim(p)} \times \mathbb{R}^{\dim(d)} \to \mathbb{R}^{\dim(g)}$ is a set of constraint functions. Represent the constraint violation set at design point $\boldsymbol{d}$ by*

$$\mathcal{F}(\boldsymbol{d}, \boldsymbol{g}) = \bigcup_{i=1}^{\dim(\boldsymbol{g})} \mathcal{F}_i(\boldsymbol{d}, \boldsymbol{g}), \tag{1}$$

where, for $1 \leq i \leq \dim(\boldsymbol{g})$,

$$\mathcal{F}_i(\boldsymbol{d}, \boldsymbol{g}) = \left\{\boldsymbol{p} \in \mathbb{R}^{\dim(\boldsymbol{p})} : \boldsymbol{g}_i(\boldsymbol{p}, \boldsymbol{d}) > 0\right\}. \tag{2}$$

When the arguments $\boldsymbol{d}$ *and* $\boldsymbol{g}$ *are understood from context, they will be omitted.*

Notation. Recall that a point is a *boundary point* of a set if every neighborhood of the point touches both the set and its complement. The *boundary* of the set is the set of all its boundary points. The symbol ∂ represents the topological boundary operator; i.e., if A is a set, ∂A is its set of boundary points.

Lemma 1. *Let* $\boldsymbol{d}$ *be a fixed design. Suppose that the constraint set* $\boldsymbol{g} : \mathbb{R}^{\dim(\boldsymbol{p})} \times \mathbb{R}^{\dim(\boldsymbol{d})} \to \mathbb{R}^{\dim(\boldsymbol{g})}$ *is composed of continuous functions of* $\boldsymbol{p}$ *for a fixed* $\boldsymbol{d}$*. If* $\boldsymbol{p} \in \partial\mathcal{F}$, $\boldsymbol{g}_i(\boldsymbol{p}, \boldsymbol{d}) = 0$ *for some* i.

Proofs are provided in the Appendix.

Remark. The converse of this Lemma is not true. That is to say, if $\boldsymbol{g}_i(\boldsymbol{p}, \boldsymbol{d}) = 0$ for some i, it does not follow with mathematical certainty that $\boldsymbol{p} \in \partial\mathcal{F}$. For example, if $\dim(\boldsymbol{g}) = 1$ and $\boldsymbol{g}_1(\boldsymbol{p}, \boldsymbol{d}) \triangleq (\boldsymbol{p}_1 - 1)^2(\boldsymbol{p}_1 - 2)$, any $\boldsymbol{p}^*$ with $\boldsymbol{p}_1^* = 1$ has $\boldsymbol{g}_1(\boldsymbol{p}^*, \boldsymbol{d}) = 0$, but all $\boldsymbol{p} \in \mathcal{F}_1$ must have $\boldsymbol{p}_1 > 2$, so $\boldsymbol{p}^* \notin \partial\mathcal{F}$.

Constructing this counterexample required creating the juxtaposition of mathematical events; in this case, a constraint function achieved the transition value of 0 between feasibility and infeasibility while at the same point its gradient also became 0. We believe that, in a realistic engineering setting, this is unlikely. So, this counterexample notwithstanding, we will assume in this paper that the boundary of each constraint function violation region $\mathcal{F}_i$ is exactly described by the points where that constraint function has value zero; i.e.,

$$\partial\mathcal{F}_i(\boldsymbol{d}, \boldsymbol{g}) = \{\boldsymbol{p} : \boldsymbol{g}_i(\boldsymbol{p}, \boldsymbol{d}) = 0\}. \tag{3}$$

We expect that there is little loss of generality in making this assumption. This assumption provides a formula for $\partial\mathcal{F}_i$.

Definition 4 (Critical Similitude Ratio (CSR)). *Let* $\boldsymbol{d}$ *be a fixed design and let* $\Delta_{\boldsymbol{p}}$ *and* $\bar{\boldsymbol{p}}$ *be the support set and designated point of the uncertainty model of* $\boldsymbol{p}$*. The set of expansion/contraction factors which produce homothets of* $\Delta_{\boldsymbol{p}}$ *with respect to* $\bar{\boldsymbol{p}}$ *which contain points in the failure region is denoted*

$$\tilde{A}(\bar{\boldsymbol{p}}, \Delta_{\boldsymbol{p}}, \boldsymbol{d}, \boldsymbol{g}) \triangleq \left\{\alpha \geq 0 : \mathcal{H}(\Delta_{\boldsymbol{p}}, \bar{\boldsymbol{p}}, \alpha) \bigcap \mathcal{F}(\boldsymbol{d}, \boldsymbol{g}) \neq \emptyset\right\}. \tag{4}$$

The greatest lower bound (also called infimum*) of* $\tilde{A}(\bar{\boldsymbol{p}}, \Delta_{\boldsymbol{p}}, \boldsymbol{d}, \boldsymbol{g})$*, represented by*

$$\tilde{\alpha}(\bar{\boldsymbol{p}}, \Delta_{\boldsymbol{p}}, \boldsymbol{d}, \boldsymbol{g}) \triangleq \inf\left(\tilde{A}(\bar{\boldsymbol{p}}, \Delta_{\boldsymbol{p}}, \boldsymbol{d}, \boldsymbol{g})\right), \tag{5}$$

will be called the Critical Similitude Ratio. When the arguments $\bar{\boldsymbol{p}}$, $\Delta_{\boldsymbol{p}}$, $\boldsymbol{d}$, *and* $\boldsymbol{g}$ *are understood from context, they will be omitted.*

Remark. Standard mathematical convention is that the greatest lower bound of the empty set is ∞. This is consistent with the proper value for $\tilde{\alpha}$ in case $\tilde{A}$ is empty.

Lemma 2 (Properties). *Let $\boldsymbol{d}$ be a fixed design and let $\Delta_{\boldsymbol{p}}$ and $\bar{\boldsymbol{p}}$ be the support set and designated point of the uncertainty model of $\boldsymbol{p}$. Suppose that $\boldsymbol{g} : \mathbb{R}^{\dim(\boldsymbol{p})} \times \mathbb{R}^{\dim(\boldsymbol{d})} \rightarrow \mathbb{R}^{\dim(\boldsymbol{g})}$ is a set of constraint functions. This Lemma considers possible consequences of the following hypotheses:*

*i. The uncertainty set $\Delta_{\boldsymbol{p}}$ is a closed and bounded set (*a.k.a. *a compact set).*

ii. The constraint functions $\boldsymbol{g}(\boldsymbol{p}, \boldsymbol{d})$ are continuous functions of $\boldsymbol{p}$ for the fixed $\boldsymbol{d}$.

iii. The designated point $\bar{\boldsymbol{p}}$ is an interior *point of $\Delta_{\boldsymbol{p}}$.*

iv. The constraints are violated at some point; i.e., $\mathcal{F} \neq \emptyset$.

v. The constraints are strongly *satisfied at the designated point; i.e., $\boldsymbol{g}(\bar{\boldsymbol{p}}, \boldsymbol{d}) < 0$.*

The following conclusions may be drawn:

a. (i), (ii), & (v) $\Rightarrow\ 0 < \tilde{\alpha}$.

b. (iii) & (iv) $\Rightarrow\ \tilde{\alpha} < \infty$.

c. (ii) & $(0 < \tilde{\alpha})\ \Rightarrow \mathcal{H}(\Delta_{\boldsymbol{p}}, \bar{\boldsymbol{p}}, \tilde{\alpha}) \bigcap \mathcal{F} = \emptyset$.

d. (i), (ii) & $(0 < \tilde{\alpha} < \infty)\ \Rightarrow \partial\mathcal{H}(\Delta_{\boldsymbol{p}}, \bar{\boldsymbol{p}}, \tilde{\alpha}) \cap \partial\mathcal{F} \neq \emptyset$.

Remarks. At least under the hypotheses (i), (ii), and (v), $\mathcal{H}(\Delta_{\boldsymbol{p}}, \bar{\boldsymbol{p}}, \tilde{\alpha})$ is the homothetic expansion (or, perhaps, contraction) of $\Delta_{\boldsymbol{p}}$ which, starting from a contraction so small that it contains no constraint violation points, has grown as large as possible without encroaching on the constraint violation region. Conclusion (a) asserts conditions under which $\mathcal{H}(\Delta_{\boldsymbol{p}}, \bar{\boldsymbol{p}}, \tilde{\alpha})$ is not trivially small (the single point $\bar{\boldsymbol{p}}$). Conclusion (b) asserts conditions under which *some* homothet $\mathcal{H}(\Delta_{\boldsymbol{p}}, \bar{\boldsymbol{p}}, \alpha)$ of $\Delta_{\boldsymbol{p}}$ touches the constraint violation region. Conclusion (c) gives conditions under which no point of $\mathcal{H}(\Delta_{\boldsymbol{p}}, \bar{\boldsymbol{p}}, \tilde{\alpha})$ violates any constraint. Conclusion (d) gives conditions under which a CPV exists; see Definition (5).

Definition 5 (Critical Parameter Value (CPV)). *Let $\boldsymbol{d}$ be a given design and let $\Delta_{\boldsymbol{p}}$, $\bar{\boldsymbol{p}}$, and $\boldsymbol{g}$ be as stated in Lemma 2. Any $\tilde{\boldsymbol{p}}$ lying in $\partial\mathcal{H}(\Delta_{\boldsymbol{p}}, \bar{\boldsymbol{p}}, \tilde{\alpha}) \cap \partial\mathcal{F}$ will be called a Critical Parameter Value for this design, uncertainty model, and constraint set.*

By Lemma 2(d), whenever $\Delta_{\boldsymbol{p}}$ is compact, the components of $\boldsymbol{g}$ are continuous functions, and some homothet of $\Delta_{\boldsymbol{p}}$ with positive similitude ratio is disjoint from the constraint violation set, the existence of a CPV is guaranteed. Note also that the CPV might not be a realization of the uncertain parameter; i.e., $\tilde{\boldsymbol{p}}$ might not belong to $\Delta_{\boldsymbol{p}}$. Further note that the CPV might not be uniquely determined; i.e., $\partial\mathcal{H}(\Delta_{\boldsymbol{p}}, \bar{\boldsymbol{p}}, \tilde{\alpha}) \cap \partial\mathcal{F}$ might contain several points. Figures 1 and 2 show sketches with relevant metrics for hyper-spherical and hyper-rectangular supports respectively.

Definition 6 (Feasible Design Space (FDS)). *The* Feasible Design Space *(FDS) is the set of designs satisfying all the constraints at the designated point.*

Definition 7 (Robust Design Space (RDS)). *The* Robust Design Space *(RDS) is the set of designs satisfying the hard constraints for all points of the uncertainty set of a given uncertainty model. Each member of the RDS set is called a* Robust Design.

Note that if the RDS exists, it is a subset of the FDS.

Formal definitions of the PSM for hyper-spherical and hyper-rectangular supports are provided in Section IV, as are expressions for the calculation of these PSMs. In general, the PSM is uniquely specified by the design point $\boldsymbol{d}$, the support set $\Delta_{\boldsymbol{p}}$, the designated point $\bar{\boldsymbol{p}}$, the constraint functions $\boldsymbol{g}$, and the CSR $\tilde{\alpha}$. The PSM is proportional to the degree of robustness of $\boldsymbol{d}$ to uncertainty in $\boldsymbol{p}$ for a given geometry of the uncertainty model. If the PSM assumes the value of zero, the designated point $\bar{\boldsymbol{p}}$ is on the boundary of the constraint violation region. This means that there is no robustness to uncertainty in $\boldsymbol{p}$ since at least one of the constraints is active for $\bar{\boldsymbol{p}}$, i.e., there exist arbitrarily small perturbations of $\boldsymbol{p}$ from $\bar{\boldsymbol{p}}$ leading to a constraint violation. The PSM assumes non-negative values in the FDS. Negative PSM values are attained by designs outside the FDS.

IV. Robustness Analysis

Problem Statement: Does the design $\boldsymbol{d}$ satisfy the hard constraints $\boldsymbol{g}(\boldsymbol{p},\boldsymbol{d}) \leq \boldsymbol{0}$ for each $p \in \Delta_{\boldsymbol{p}}$?

The uncertainty set can have arbitrary shape, size and connectivity. However, when the uncertainty model is more restricted in its structure a simple test for robustness can be established. We recall a definition from mathematical convexity theory.

Definition 8 (Star Convexity[12]). *The set A is* star convex *with respect to a point x if, for each $a \in A$, the entire line segment connecting a and x is a subset of A.*

The five pointed star as used, for example, on the United States flag, is not convex, but is star convex with respect to its geometric center.

A property related to homothetic expansion and contraction of uncertainty models is introduced next.

Definition 9 (Homothetic Monotonicity). *An uncertainty model $\langle \Delta_{\boldsymbol{p}}, \bar{\boldsymbol{p}} \rangle$ is said to be homotheticly monotone if, whenever $0 \leq \alpha_1 < \alpha_2$, it is also true that $\mathcal{H}(\Delta_{\boldsymbol{p}}, \bar{\boldsymbol{p}}, \alpha_1) \subset \mathcal{H}(\Delta_{\boldsymbol{p}}, \bar{\boldsymbol{p}}, \alpha_2)$.*

An example of a set which is not homotheticly monotone is a set shaped like a capital "S" with its designated point at the inflection point. Note that all convex sets, including hyper-spheres and hyper-rectangles, are homotheticly monotone with respect to any of their points. These two notions are intimately connected.

Lemma 3. *The uncertainty model $\langle \Delta_{\boldsymbol{p}}, \bar{\boldsymbol{p}} \rangle$ is homotheticly monotone if and only if $\Delta_{\boldsymbol{p}}$ is star convex with respect to $\bar{\boldsymbol{p}}$.*

So, while it will be more natural in the context of the present work to view this property as homothetic monotonicity, it is seen to be an equivalent restatement of the standard mathematical notion of star convexity.

For uncertainty models with this structure, the following robustness test can be applied.

Lemma 4 (Robustness Test). *Let $\langle \Delta_{\boldsymbol{p}}, \bar{\boldsymbol{p}} \rangle$ be a homotheticly monotone uncertainty model such that $\Delta_{\boldsymbol{p}}$ is compact. Let $\boldsymbol{d}$ be a fixed design point and let the constraint functions $\boldsymbol{g}(\boldsymbol{p}, \boldsymbol{d})$ be continuous functions of $\boldsymbol{p}$. Suppose that the CSR $\tilde{\alpha}$ satisfies $0 < \tilde{\alpha} < \infty$. Then the design $\boldsymbol{d}$ is robust if and only if $\tilde{\alpha} \geq 1$.*

Remark. The significance of the lower bound 1 for $\tilde{\alpha}$ is that $\mathcal{H}(\Delta_{\boldsymbol{p}}, \bar{\boldsymbol{p}}, 1) = \Delta_{\boldsymbol{p}}$.

Implementing this test to establish robustness of a design is facilitated by the calculation of the CSR and a CPV. For this, it helps to restrict the geometry of the uncertainty model a little more. To this end, we have created the following variation on the notion of star convexity:

Definition 10 (Strict Star Convexity). *The set A is* strictly star convex *with respect to a point $x \in A$ if, for each $a \in A$, every interior point of the segment connecting a and x is an interior point of A.*

For example, all hyper-spheres and hyper-rectangles are strictly star convex with respect to any of their *interior* points. For an uncertainty model which is strictly star convex with respect to its designated point, alternate expressions for the CSR are presented next since they will be useful in numerical calculations.

Lemma 5 (Alternate CSR Expressions). *If $\langle \Delta_{\boldsymbol{p}}, \bar{\boldsymbol{p}} \rangle$ is an uncertainty model for which $\Delta_{\boldsymbol{p}}$ is closed, bounded, and strictly star convex with respect to $\bar{\boldsymbol{p}}$ and $\bar{\boldsymbol{p}}$ is an* interior *point of $\Delta_{\boldsymbol{p}}$, and, for the fixed design point $\boldsymbol{d}$, the constraint functions $\boldsymbol{g}$ are continuous functions of $\boldsymbol{p}$, and the CSR $\tilde{\alpha}$ satisfies $0 < \tilde{\alpha} < \infty$, the following are alternate characterizations of $\tilde{\alpha}$:*

$$\tilde{\alpha} = \min \left\{ \alpha : \mathcal{H}(\Delta_{\boldsymbol{p}}, \bar{\boldsymbol{p}}, \alpha) \bigcap \overline{\mathcal{F}} \neq \emptyset \right\} \tag{6}$$

$$\tilde{\alpha} = \min \left\{ \alpha : \partial\mathcal{H}(\Delta_{\boldsymbol{p}}, \bar{\boldsymbol{p}}, \alpha) \bigcap \left[\bigcup_{k=1}^{\dim(\boldsymbol{g})} \partial\mathcal{F}_k \right] \neq \emptyset \right\} \tag{7}$$

$$\tilde{\alpha} = \min_{1 \leq k \leq \dim(\boldsymbol{g})} \left[\min \left\{ \alpha : \partial\mathcal{H}(\Delta_{\boldsymbol{p}}, \bar{\boldsymbol{p}}, \alpha) \bigcap \partial\mathcal{F}_k \neq \emptyset \right\} \right] \tag{8}$$

$$\tilde{\alpha} = \min_{1 \leq k \leq \dim(\boldsymbol{g})} \left[\min \left\{ \alpha : \partial\mathcal{H}(\Delta_{\boldsymbol{p}}, \bar{\boldsymbol{p}}, \alpha) \bigcap \overline{\mathcal{F}_k} \neq \emptyset \right\} \right] \tag{9}$$

where $\overline{\mathcal{F}} = \mathcal{F} \bigcup \partial\mathcal{F}$ is the topological closure of $\mathcal{F}$.

Remarks.

1. In this lemma, the hypothesis of strict star convexity cannot be weakened to simply star convexity.

2. Recall that the mathematical statement "$x = \min A$" is a shorthand for the two assertions "$x = \inf A$" and "$x \in A$".

3. Compare Equation (6) with

$$\tilde{\alpha} = \inf_{\alpha} \left\{ \alpha : \mathcal{H}(\Delta_{\boldsymbol{p}}, \bar{\mathbf{p}}, \alpha) \bigcap \mathcal{F} \neq \emptyset \right\}$$

which is a restatement of Definition 4.

4. Compare Equation (7) with Lemma 2(d) which uses the (in general) smaller boundary set $\partial\mathcal{F}$.

5. The assumption in Equation (3) motivates the inclusion of the characterization of $\tilde{\alpha}$ in Equation (8).

The calculation of the CSR and a CPV can now be stated in the form of an optimization problem.

Lemma 6 (CSR and CPV calculation). *If $\langle \Delta_{\boldsymbol{p}}, \bar{\mathbf{p}} \rangle$ is an uncertainty model for which $\Delta_{\boldsymbol{p}}$ is closed, bounded, and strictly star convex with respect to $\bar{\mathbf{p}}$ and $\bar{\mathbf{p}}$ is an* interior *point of $\Delta_{\boldsymbol{p}}$, and, for the fixed design point $\mathbf{d}$, the constraint functions $\boldsymbol{g}$ are continuous functions of $\mathbf{p}$, and the CSR $\tilde{\alpha}$ satisfies $0 < \tilde{\alpha} < \infty$, the following are optimization characterizations of the CPV $\tilde{\mathbf{p}}$ and the CSR $\tilde{\alpha}$:*

$$\langle \tilde{\boldsymbol{p}}, \tilde{\alpha} \rangle = \operatorname*{argmin}_{\langle \boldsymbol{p}, \alpha \rangle} \left\{ \alpha : \boldsymbol{p} \in \mathcal{H}(\Delta_{\boldsymbol{p}}, \bar{\boldsymbol{p}}, \alpha) \bigcap \overline{\mathcal{F}} \right\}; \tag{10}$$

$$\langle \tilde{\boldsymbol{p}}, \tilde{\alpha} \rangle = \operatorname*{argmin}_{\langle \boldsymbol{p}, \alpha \rangle} \left\{ \alpha : \boldsymbol{p} \in \partial\mathcal{H}(\Delta_{\boldsymbol{p}}, \bar{\boldsymbol{p}}, \alpha) \bigcap \left[\bigcup_{k=1}^{\dim(\boldsymbol{g})} \partial\mathcal{F}_k \right] \right\}; \tag{11}$$

$$\begin{aligned} \langle \tilde{\boldsymbol{p}}, \tilde{\alpha} \rangle &= \langle \tilde{\boldsymbol{p}}^{(n)}, \tilde{\alpha}_n \rangle, \\ &\textit{where } n = \operatorname*{argmin}_{1 \le k \le \dim(\boldsymbol{g})} \{\tilde{\alpha}_k\}, \textit{ and, for } 1 \le k \le \dim(\boldsymbol{g}), \\ &\langle \tilde{\boldsymbol{p}}^{(k)}, \tilde{\alpha}_k \rangle = \operatorname*{argmin}_{\langle \boldsymbol{p}, \alpha \rangle} \left\{ \alpha : \boldsymbol{p} \in \partial\mathcal{H}(\Delta_{\boldsymbol{p}}, \bar{\boldsymbol{p}}, \alpha) \bigcap \partial\mathcal{F}_k \right\}; \textit{ and} \end{aligned} \tag{12}$$

$$\begin{aligned} \langle \tilde{\boldsymbol{p}}, \tilde{\alpha} \rangle &= \langle \tilde{\boldsymbol{p}}^{(n)}, \tilde{\alpha}_n \rangle, \\ &\textit{where } n = \operatorname*{argmin}_{1 \le k \le \dim(\boldsymbol{g})} \{\tilde{\alpha}_k\}, \textit{ and, for } 1 \le k \le \dim(\boldsymbol{g}), \\ &\langle \tilde{\boldsymbol{p}}^{(k)}, \tilde{\alpha}_k \rangle = \operatorname*{argmin}_{\langle \boldsymbol{p}, \alpha \rangle} \left\{ \alpha : \boldsymbol{p} \in \partial\mathcal{H}(\Delta_{\boldsymbol{p}}, \bar{\boldsymbol{p}}, \alpha) \bigcap \overline{\mathcal{F}_k} \right\}. \end{aligned} \tag{13}$$

Remark. In addition to being a restatement of Lemma 5, this Lemma adds the information that any point in the non-empty sets of Lemma 5 at which the various minima are attained *is* a CPV. Recall that the notation

$$\underset{v}{\operatorname{argmin}}\{f(v) : v \in \mathcal{X}\}$$

represents the value of v at which the objective function f takes on its smallest value subject to the constraint $v \in \mathcal{X}$.

Support sets with hyper-spherical and hyper-rectangular geometries are studied next. These strategies are then used to handle supports with other geometries.

IV.A. Hyper-Spheres

Hyper-spherical support sets result from uncertainty models where uncertainty is described by norm bounded perturbations from the nominal parameter value $\bar{\boldsymbol{p}}$. This implies that $\Delta_{\boldsymbol{p}}$ is a hyper-sphere and $\bar{\boldsymbol{p}}$ is its geometric center. Problems with this class of support sets are the simplest since the CPV is calculated by solving a minimum norm problem in $\boldsymbol{p}$-space. Under the assumption in Equation (3), the CPV for $\Delta_{\boldsymbol{p}} = \mathcal{S}_{\boldsymbol{p}}(\bar{\boldsymbol{p}}, R)$ is given by

$$\tilde{\boldsymbol{p}} = \underset{\boldsymbol{p}}{\operatorname{argmin}} \left\{ \|\boldsymbol{p} - \bar{\boldsymbol{p}}\| : \prod_{k=1}^{\dim(\boldsymbol{g})} \boldsymbol{g}_k(\boldsymbol{p}, \boldsymbol{d}) = 0 \right\}. \tag{14}$$

This is the application of Lemma 6, Equation (11) to this particular $\Delta_{\boldsymbol{p}}$. The condition $\boldsymbol{p} \in \partial\mathcal{H}(\Delta_{\boldsymbol{p}}, \bar{\boldsymbol{p}}, \alpha)$ becomes $\|\boldsymbol{p} - \bar{\boldsymbol{p}}\| = \alpha R$. Under the assumption in Equation (3), the constraint above is a restatement of the requirement that $\boldsymbol{p} \in \cup_{k=1}^{\dim(\boldsymbol{g})} \partial\mathcal{F}_k$. Because of the difficulty which the constraint $\prod_{k=1}^{\dim(\boldsymbol{g})} \boldsymbol{g}_k(\boldsymbol{p}, \boldsymbol{d}) = 0$ would present to standard gradient based numerical optimization software (at any point where two or more of the constraints are zero, the gradient of $\prod_{k=1}^{\dim(\boldsymbol{g})} \boldsymbol{g}_k(\boldsymbol{p}, \boldsymbol{d}) = 0$ also vanishes), the formula for the CPV $\tilde{\boldsymbol{p}}$ is restated in the Lemma 6, Equation (12), form:

$$\tilde{\boldsymbol{p}} = \tilde{\boldsymbol{p}}^{(n)}, \tag{15}$$

where

$$n = \underset{1 \le k \le \dim(\boldsymbol{g})}{\operatorname{argmin}} \left\{ \|\tilde{\boldsymbol{p}}^{(k)} - \bar{\boldsymbol{p}}\| \right\}, \tag{16}$$

and, for each k with $1 \le k \le \dim(\boldsymbol{g})$,

$$\tilde{\boldsymbol{p}}^{(k)} = \underset{\boldsymbol{p}}{\operatorname{argmin}} \left\{ \|\boldsymbol{p} - \bar{\boldsymbol{p}}\| : \boldsymbol{g}_k(\boldsymbol{p}, \boldsymbol{d}) = 0 \right\}. \tag{17}$$

That is, the CPV problem is solved for each individual constraint function, and the answer is selected which is closest to the designated point. By applying Lemma 6, Equation (10) or Equation (13), in the preceding, we see that the equality constraints may be replaced by the inequality constraints $\prod_{k=1}^{\dim(\boldsymbol{g})} \boldsymbol{g}_k(\boldsymbol{p}, \boldsymbol{d}) \geq 0$ and $\boldsymbol{g}_k(\boldsymbol{p}, \boldsymbol{d}) \geq 0$, respectively. This can be useful if the optimization algorithm being used to solve the optimization problem works better with, or even requires, inequality constraints instead of equality constraints.

Lemma 4 can be readily used once the CPV is found; since, for a hyper-spherical support set of radius R and center $\bar{\boldsymbol{p}}$, the CSR can be calculated from the CPV.

Definition 11 (Spherical PSM). *The Spherical Parametric Safety Margin corresponding to the design $\boldsymbol{d}$ for $\Delta_{\boldsymbol{p}} = \mathcal{S}_{\boldsymbol{p}}(\bar{\boldsymbol{p}}, R)$ is defined as*

$$\rho_{\mathcal{S}}(\bar{\boldsymbol{p}}, \tilde{\boldsymbol{p}}, \boldsymbol{d}) \stackrel{\Delta}{=} \|\tilde{\boldsymbol{p}} - \bar{\boldsymbol{p}}\|, \tag{18}$$

where $\bar{\boldsymbol{p}}$ is the designated point of the uncertainty model and $\tilde{\boldsymbol{p}}$ is a corresponding CPV.

Lemma 7. $\rho_{\mathcal{S}} = \tilde{\alpha} R$.

Note that $\tilde{\alpha}$ is inversely proportional to R, so that $\rho_{\mathcal{S}}$ is independent of R, i.e., if the PSM is calculated for two different spherical support sets centered at the same designated point, both calculations give the same value for the PSM. The CSR can be thought of as a non-dimensional measure of robustness to parameter uncertainty while the PSM has a value which relates to the units of the parameters in the vector $\boldsymbol{p}$.

Lemma 4 for hyper-spherical supports can now be reformulated as follows.

Lemma 8 (P-Test). *Let $\boldsymbol{g} \leq \boldsymbol{0}$ describe a set of continuous inequality constraints and $\Delta_{\boldsymbol{p}} = \mathcal{S}_{\boldsymbol{p}}(\bar{\boldsymbol{p}}, R)$ be the support of the uncertain parameter $\boldsymbol{p}$. The design $\boldsymbol{d}$ is robust if and only if $\rho_{\mathcal{S}} \geq R$.*

A sketch showing relevant quantities is displayed in Figure (1).

The exact boundary of the RDS corresponding to a hyper-spherical support set is given by an iso-spherical-PSM manifold, i.e., surface in the design space prescribed by $\rho_{\mathcal{S}} = c$, where c is a constant.

IV.B. Hyper-Rectangles

When each component of the uncertain parameter is confined to a prescribed interval, the support set is a hyper-rectangle. Note that this geometry allows for the manipulation of sets of parameters having different units and levels of fidelity. Recall that if $\bar{\boldsymbol{p}}$ is the geometric center of the hyper-rectangle, and $\boldsymbol{m}$ is the vector of half-lengths of its sides, the resulting hyper-rectangle is denoted as $\mathcal{R}_{\boldsymbol{p}}(\bar{\boldsymbol{p}}, \boldsymbol{m})$. A robustness test for supports with this geometry is introduced subsequently. The mathematical background for this is presented next. It is based on the definition of a mapping which we call a *Q-transformation* which distorts $\boldsymbol{p}$-space so that the hyper-rectangle is distorted into a sphere.

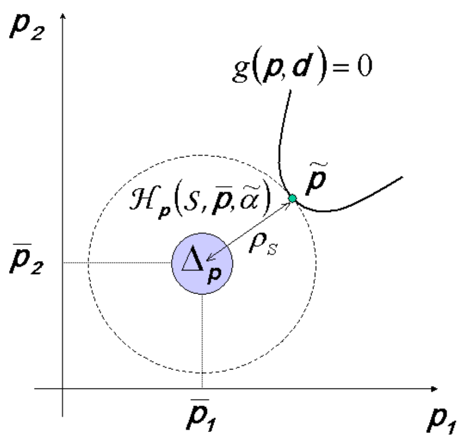

Figure 1. Relevant metrics for a circular support.

Definition 12 (Q-Transformation). *Let $\Delta_{\boldsymbol{p}} = \mathcal{R}_{\boldsymbol{p}}(\bar{\boldsymbol{p}}, \boldsymbol{m})$ be the support of the uncertain parameter $\boldsymbol{p}$. The Q-Transformation is denoted as $\boldsymbol{q} = Q(\boldsymbol{p})$ and is given by $Q(\bar{\boldsymbol{p}}) = 0$ and, for $\boldsymbol{p} \neq \bar{\boldsymbol{p}}$,*

$$\boldsymbol{q} \triangleq \frac{\max\{|\boldsymbol{k}|\}\boldsymbol{k}}{\|\boldsymbol{k}\|} \text{ where} \tag{19}$$

$$\boldsymbol{k} = \text{diag}\{\boldsymbol{m}\}^{-1}(\boldsymbol{p} - \bar{\boldsymbol{p}}), \tag{20}$$

Lemma 9 (Q-Transformation Properties). *The Q-Transformation maps $\mathcal{R}_{\boldsymbol{p}}(\bar{\boldsymbol{p}}, \boldsymbol{m})$ into a unit hyper-sphere in $\boldsymbol{q}$-space. The inverse transformation, $\boldsymbol{p} = Q^{-1}(\boldsymbol{q})$, is given by*

$$\boldsymbol{p} = \bar{\boldsymbol{p}} + \frac{\|\boldsymbol{q}\|\text{diag}\{\boldsymbol{m}\}\boldsymbol{q}}{\max\{|\boldsymbol{q}|\}}. \tag{21}$$

The proof of this Lemma is routine, and is omitted. The Q-Transform is designed to have the following properties:

1. Q is continuous at $\bar{\boldsymbol{p}}$.

2. The image under Q of a line through $\bar{\boldsymbol{p}}$ is a parallel line through $\mathbf{0}$. Distances between points on the image line are proportional to the distances between their pre-images.

3. The proportionality constant used in mapping these lines changes from one line to another in such a manner that the image under Q of $\mathcal{R}_{\boldsymbol{p}}(\bar{\boldsymbol{p}}, \boldsymbol{m})$ is exactly $\mathcal{S}_{\boldsymbol{q}}(\mathbf{0}, 1)$.

4. Q maps homothets of the hyper-rectangle to homothets of the hyper-sphere preserving similitude ratio, i.e.,

$$Q(\mathcal{H}(\mathcal{R}_{\boldsymbol{p}}(\bar{\boldsymbol{p}}, \boldsymbol{m}), \bar{\boldsymbol{p}}, \alpha)) = \mathcal{H}(\mathcal{S}_{\boldsymbol{q}}(\mathbf{0}, 1), \mathbf{0}, \alpha) = \mathcal{S}_{\boldsymbol{q}}(\mathbf{0}, \alpha).$$

Differentiable functions on $\boldsymbol{p}$-space are transformed into functions on $\boldsymbol{q}$-space which can have derivative discontinuities at points corresponding to $\boldsymbol{p}$-space points where faces of homothets of the hyper-rectangle meet.

The Q-Transformation allows identification of the corresponding CPV by solving the following minimum norm problem in $\boldsymbol{q}$-space:

$$\tilde{\boldsymbol{p}} = \underset{\boldsymbol{p}}{\operatorname{argmin}} \left\{ \|Q(\boldsymbol{p})\| : \prod_{k=1}^{\dim(\boldsymbol{g})} \boldsymbol{g}_k\left(\boldsymbol{p}, \boldsymbol{d}\right) = 0 \right\} \tag{22}$$

Under the assumption given in Equation (3), this is another application of Lemma 6, Equation (11). Equation (3) implies that $\boldsymbol{p} \in \left[\bigcup_{k=1}^{\dim(\boldsymbol{g})} \partial\mathcal{F}_k\right]$ is equivalent to $\prod_{k=1}^{\dim(\boldsymbol{g})} \boldsymbol{g}_k\left(\boldsymbol{p}, \boldsymbol{d}\right) = 0$. And, if we set $\alpha = \|Q(\boldsymbol{p})\|$, then $\boldsymbol{p} \in \partial\mathcal{H}(\Delta_{\boldsymbol{p}}, \bar{\boldsymbol{p}}, \alpha)$. This calculation must be implemented with the caveat posed following Equation (14), justified by Lemma 6, Equation (12). As before, Lemma 6, Equation (10) or Equation (13), allows us to replace equality constraints with inequality constraints.

Definition 13 (Rectangular PSM). *The Rectangular Parametric Safety Margin corresponding to the design $\boldsymbol{d}$ for $\Delta_{\boldsymbol{p}} = \mathcal{R}_{\boldsymbol{p}}(\bar{\boldsymbol{p}}, \boldsymbol{m})$, is defined as*

$$\rho_{\mathcal{R}}(\bar{\boldsymbol{p}}, \tilde{\boldsymbol{p}}, \boldsymbol{m}, \boldsymbol{d}) \stackrel{\Delta}{=} \tilde{\alpha}\|\boldsymbol{m}\|. \tag{23}$$

As always, $\mathcal{H}(\mathcal{R}, \bar{\boldsymbol{p}}, \tilde{\alpha})$ is the maximal homothet of the uncertainty model which contains no constraint violation points. The rectangular-PSM is related to the diagonal measure of this hyper-rectangle. This provides comparability between rectangular-PSMs measured, for example, for different design points and therefore different constraint geometries and different locations of the CPV. Note that $\mathcal{H}(\mathcal{R}, \bar{\boldsymbol{p}}, \tilde{\alpha})$ is inscribed in a hyper-sphere centered at $\bar{\boldsymbol{p}}$ of radius equal to its rectangular-PSM. Lemma 4 can be restated for hyper-rectangular supports as follows.

Lemma 10 (Q-Test). *Let $\boldsymbol{g} \leq \boldsymbol{0}$ describe a set of continuous inequality constraints, and $\Delta_{\boldsymbol{p}} = \mathcal{R}_{\boldsymbol{p}}(\bar{\boldsymbol{p}}, \boldsymbol{m})$ be the support of the uncertain parameter. The design $\boldsymbol{d}$ is robust if and only if $\|\tilde{\boldsymbol{q}}\| \geq 1$, where $\tilde{\boldsymbol{q}} \stackrel{\Delta}{=} Q(\tilde{\boldsymbol{p}})$; i.e. $\rho_{\mathcal{R}} \geq \|\boldsymbol{m}\|$.*

A sketch showing relevant quantities is displayed in Figure (2). Note that $\hat{\boldsymbol{p}} = \bar{\boldsymbol{p}} + \tilde{\alpha}\boldsymbol{m}$ and $\hat{\boldsymbol{q}} = Q(\hat{\boldsymbol{p}})$, so $\hat{\boldsymbol{q}} = \tilde{\alpha} \cdot \boldsymbol{1}$ is the vector all of whose components are $\tilde{\alpha}$. Recall that the CPVs in Equations (14) and (22) are $\boldsymbol{p}$ values, not necessarily realizations in $\Delta_{\boldsymbol{p}}$, on the surface of a hyper-sphere and a hyper-rectangle at the verge of violating at least one of the constraints. As before, the boundary of the RDS is given by an iso-rectangular-PSM manifold.

Throughout this paper the designated point $\bar{\boldsymbol{p}}$ is chosen to be the geometric center of the support set. This however, might not always be desirable. For instance, if the uncertain variables are strictly positive, by placing the designated point on the surface of the support set, dilations to the negative $\boldsymbol{p}$ subspace can be prevented in the search for the CPV.

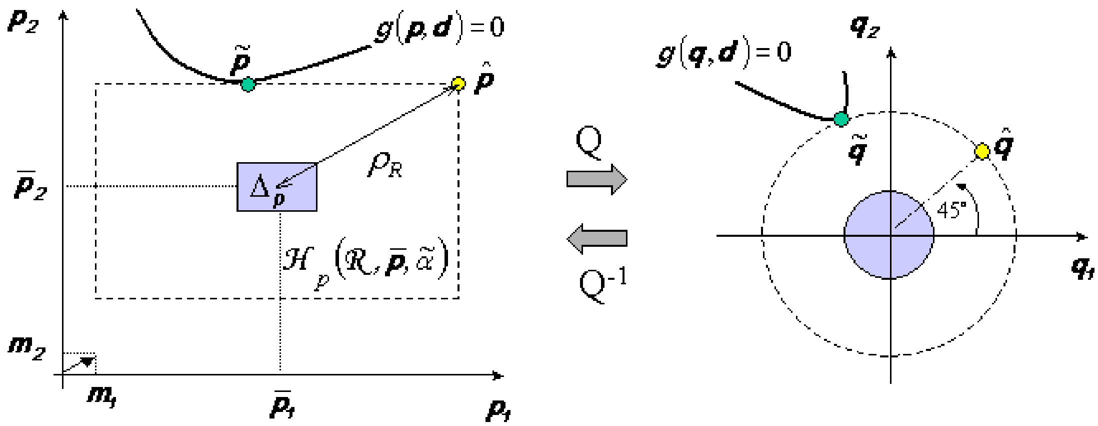

Figure 2. Relevant metrics for a rectangular support.

Infinity Norm Formulation

An alternative way to search for the CPV for hyper-rectangular supports is presented here. This formulation allows us to circumvent the problems caused by discontinuities in the gradient of the Q-Transformation.

Recall that the infinity norm in a finite dimensional space is defined as $\|\boldsymbol{x}\|^{\infty} = \sup_i\{|\boldsymbol{x}_i|\}$. Let us define the $\boldsymbol{m}$-scaled infinity norm as $\|\boldsymbol{x}\|^{\infty}_{\boldsymbol{m}} = \sup_i\{|\boldsymbol{x}_i|/\boldsymbol{m}_i\}$. A distance between the vectors $\boldsymbol{x}$ and $\boldsymbol{y}$ can be defined as $\|\boldsymbol{x}-\boldsymbol{y}\|^{\infty}_{\boldsymbol{m}}$. Using this distance, the unit ball centered at $\bar{\boldsymbol{p}}$ is just $\mathcal{R}(\bar{\boldsymbol{p}},\boldsymbol{m})$.

The problem of finding, for a fixed design $\boldsymbol{d}$, the CPV for the vector $\boldsymbol{g}(\boldsymbol{p},\boldsymbol{d})$ of constraint functions and the uncertainty model with designated point $\bar{\boldsymbol{p}}$ becomes the problem of finding a vector $\tilde{\boldsymbol{p}}$ of minimal distance in this $\boldsymbol{m}$-scaled infinity norm from $\bar{\boldsymbol{p}}$ such that $\boldsymbol{p}$ touches the failure set. This can be expressed in the form of a constrained optimization problem

$$\tilde{\boldsymbol{p}} = \underset{\boldsymbol{p}}{\operatorname{argmin}}\,\{\|\boldsymbol{p}-\bar{\boldsymbol{p}}\|^{\infty}_{\boldsymbol{m}} : \boldsymbol{p}\in\partial\mathcal{F}\}$$

This optimization problem is restated as $\tilde{\boldsymbol{p}} = \tilde{\boldsymbol{p}}^{(n)}$ where

$$n = \underset{k}{\operatorname{argmin}}\left\{\|\tilde{\boldsymbol{p}}^{(k)}-\bar{\boldsymbol{p}}\|^{\infty}_{\boldsymbol{m}}\right\}, \tag{24}$$

$$\tilde{\boldsymbol{p}}^{(k)} = \underset{\boldsymbol{p}}{\operatorname{argmin}}\,\{\|\boldsymbol{p}-\bar{\boldsymbol{p}}\|^{\infty}_{\boldsymbol{m}} : \boldsymbol{p}\in\partial\mathcal{F}_k\}. \tag{25}$$

That is, the CPV problem is solved for each individual constraint function, and the answer is selected which is closest to the designated point in the $\boldsymbol{m}$-scaled infinity norm. It should be pointed out that, in the preceding discussion, if the $\boldsymbol{m}$-scaled infinity norm is replaced by the standard Euclidean norm, what results is a formulation of the CPV calculation for spherical support sets.

Assuming that $\boldsymbol{g}(\bar{\boldsymbol{p}}, \boldsymbol{d}) < 0$ and $\partial\mathcal{F}_k = \{\boldsymbol{p} : \boldsymbol{g}_k(\boldsymbol{p}, \boldsymbol{d}) = 0\}$, the problem in Equation (25) can be formulated as

$$\tilde{\boldsymbol{p}}^{(k)} = \underset{\boldsymbol{p}}{\operatorname{argmin}}\{\|\boldsymbol{p} - \bar{\boldsymbol{p}}\|_{\boldsymbol{m}}^{\infty} : \boldsymbol{g}_k(\boldsymbol{p}, \boldsymbol{d}) = 0\}.$$

Rewriting this using the definition of the $\boldsymbol{m}$-scaled infinity norm gives

$$\tilde{\boldsymbol{p}}^{(k)} = \underset{\boldsymbol{p}}{\operatorname{argmin}}\left\{\max_{1\leq i\leq \dim(\boldsymbol{p})} \frac{|\boldsymbol{p}_i - \bar{\boldsymbol{p}}_i|}{\boldsymbol{m}_i} : \boldsymbol{g}_k(\boldsymbol{p}, \boldsymbol{d}) = 0\right\}.$$

The "max" can be eliminated and the objective function made differentiable by introducing the similitude ratio α defined earlier

$$\langle\tilde{\boldsymbol{p}}^{(k)}, \tilde{\alpha}_k\rangle = \underset{\boldsymbol{p},\alpha}{\operatorname{argmin}}\{\alpha : \boldsymbol{g}_k(\boldsymbol{p}, \boldsymbol{d}) = 0, |\boldsymbol{p}_i - \bar{\boldsymbol{p}}_i| \leq \alpha\boldsymbol{m}_i, 1 \leq i \leq \dim(\boldsymbol{p})\}.$$

This eliminates non-differentiabilities in the objective functions. The problem is turned into an "inequality constraint only" optimization problem which is more "optimizer friendly" by changing the constraint on $\boldsymbol{g}_k$ from $\boldsymbol{g}_k = 0$ to $\boldsymbol{g}_k \geq 0$ (assuming that the constraint functions $\boldsymbol{g}$ are continuous) since the optimum must occur on $\partial\mathcal{F}_k$. If n is given by (24) and $\tilde{\alpha} = \tilde{\alpha}^{(n)}$, $\tilde{\boldsymbol{p}} = \tilde{\boldsymbol{p}}^{(n)}$ is the CPV and $\mathcal{R}_{\boldsymbol{p}}(\bar{\boldsymbol{p}}, \tilde{\alpha}\boldsymbol{m})$ is the largest hyper-rectangle proportional to $\mathcal{R}_{\boldsymbol{p}}(\bar{\boldsymbol{p}}, \boldsymbol{m})$ which fits inside the non-failure region of the $\boldsymbol{p}$-space for $\boldsymbol{d}$. Another interpretation is that $\tilde{\alpha}$ is the radius of the largest unit sphere (in the $\boldsymbol{m}$-scaled infinity norm metric) centered at $\bar{\boldsymbol{p}}$ which fits inside the $\boldsymbol{p}$-space feasible set for the given design $\boldsymbol{d}$.

IV.C. Bounding Sets

We next look at how the techniques developed so far can be leveraged to provide robustness tests for support sets with other geometries. The tests and margins above enable a rigorous assessment of hyper-spherical and hyper-rectangular sets. In this section we use these geometries as bounding sets of support sets having arbitrary shapes. Studies on the bounding sets will be used to infer properties of the support set. Evidently, conservatism is unavoidably introduced since the design requirements apply to the actual support set, not to the bounding set.

Lemma 11 (Bounding Test). *Let the support set $\Delta_{\boldsymbol{p}}$ be of arbitrary shape. Define an outer bounding set $\mathcal{O}_{\boldsymbol{p}}$ as one satisfying $\Delta_{\boldsymbol{p}} \subseteq \mathcal{O}_{\boldsymbol{p}}$. If the design $\boldsymbol{d}$ satisfies the hard constraints for the bounding set $\mathcal{O}_{\boldsymbol{p}}$, the design $\boldsymbol{d}$ satisfies the hard constraints for $\Delta_{\boldsymbol{p}}$; i.e., the design is robust. On the other hand, if the design $\boldsymbol{d}$ does not satisfy the hard constraints for as much as one realization $\boldsymbol{p} \in \Delta_{\boldsymbol{p}}$, the design $\boldsymbol{d}$ does not satisfy the hard constraints for $\Delta_{\boldsymbol{p}}$; i.e., the design is not robust.*

The P- and the Q-tests can be used to assess the robustness of hyper-spherical and hyper-rectangular bounding sets respectively. Obviously, conservatism is reduced by using tighter bounding sets. Constraint violations caused by parameter values in the intersection between $\mathcal{O}_{\boldsymbol{p}}$ and the complement set of $\Delta_{\boldsymbol{p}}$ might cause a robust design to fail the Bounding Test. A conservative approximation to the RDS corresponding to $\Delta_{\boldsymbol{p}}$ is given by an iso-PSM manifold. For instance, if $\mathcal{O}_{\boldsymbol{p}} = \mathcal{S}_{\boldsymbol{p}}(\bar{\boldsymbol{p}}, R_{out})$, the design set determined by $\rho_{\mathcal{S}} \geq R_{out}$ is a subset of the actual RDS.

IV.D. Converse Case

Thus far we have only considered the case in which the designated point satisfies all the constraints in $\boldsymbol{g}$. An extension to the converse case, for which $\boldsymbol{g}(\bar{\boldsymbol{p}}, \boldsymbol{d})$ has at least one positive component, is introduced next. One situation in which a need for this extension might arise is if an automated, optimization driven design procedure varies the design parameter so much that constraint boundaries move enough to make $\bar{\boldsymbol{p}}$ a constraint violation point. If $\bar{\boldsymbol{p}} \in \mathcal{F}^c$ (where the super-script c denotes the set complement operator), the CPV for hyper-spherical support sets is given by

$$\begin{aligned} \tilde{\boldsymbol{p}} &= \underset{\boldsymbol{p}}{\operatorname{argmin}} \left\{ \|\boldsymbol{p} - \bar{\boldsymbol{p}}\| : \boldsymbol{p} \in \mathcal{F}^c \right\}, \\ &= \underset{\boldsymbol{p}}{\operatorname{argmin}} \left\{ \|\boldsymbol{p} - \bar{\boldsymbol{p}}\| : \boldsymbol{g}_i(\boldsymbol{p}, \boldsymbol{d}) \leq 0, \quad i = 1, \cdots, \dim(\boldsymbol{g}) \right\}. \end{aligned} \tag{26}$$

Expressions for hyper-rectangular support sets are obtained by using $\|Q(\boldsymbol{p})\|$ instead of $\|\boldsymbol{p} - \bar{\boldsymbol{p}}\|$ in Equation (26). The corresponding PSMs result from multiplying the right hand side of Equations (18) and (23) by minus one. Therefore, designs outside the FDS will have negative PSMs. Results must be interpreted accordingly.

Whereas hard constraints are required to be satisfied for all values of the uncertain parameters in the support set, soft constraints are only required to be satisfied for most such values. Metrics are introduced to quantify this idea. For example, the uncertain parameters could be modeled as random variables of given distributions, and restrictions could be placed on the probability of constraint violation. Numerical techniques typically used to handle soft constraints, such as sampling and reliability methods, are unable to provide conclusive solutions to the problem statement which opens section IV. Tools for handling soft constraints are based on the estimation of the probability of constraint violation. To satisfy hard constraints, this probability must be zero. Sampling-based methods can wrongly predict zero failure probabilities as a result of using a finite number of samples. On the other hand, methods based on asymptotic approximations such as FORM and SORM,[13] will not converge since the limit state in the standard normal space does not exist. Notice that PSMs allow for the unbiased comparison of the robustness characteristics of competing design alternatives. Such a comparison does not require a unifying constraint structure, i.e. the design variables as well as the way in which the constraints depend on them might be different.

V. Robust-Design

Problem Statement: For a given uncertainty set $\Delta_{\boldsymbol{p}}$ and a given designated point $\bar{\boldsymbol{p}}$, find a design $\boldsymbol{d}^*$ which is robust for as large as possible an uncertainty model proportional to $\langle \Delta_{\boldsymbol{p}}, \bar{\boldsymbol{p}} \rangle$; i.e., a design $\boldsymbol{d}^*$ whose CSR $\tilde{\alpha}^*$ is as large as possible. The set $\mathcal{M} \triangleq \mathcal{H}(\Delta_{\boldsymbol{p}}, \bar{\boldsymbol{p}}, \tilde{\alpha}^*)$ is the largest expansion (or, perhaps, contraction) of $\Delta_{\boldsymbol{p}}$ about $\bar{\boldsymbol{p}}$ for which a design can be found with the property that $\mathcal{M}$ is disjoint from the constraint violation set of this design. $\mathcal{M}$ can be called the *Maximal Feasible Homothet of the Support Set*, or *Maximal Homothet* for short. If $\Delta_{\boldsymbol{p}}$ were a hyper-sphere or hyper-rectangle with $\bar{\boldsymbol{p}}$ at its center, it follows from Lemma 7 or Definition 13, respectively, that $\mathcal{M}$ can be equivalently characterized as arising from a design $\boldsymbol{d}^*$ whose PSM is as large as possible. This problem can be posed as follows:

$$\mathcal{M}(\Delta_{\boldsymbol{p}}, \bar{\boldsymbol{p}}, \boldsymbol{g}) \triangleq \mathcal{H}(\Delta_{\boldsymbol{p}}, \bar{\boldsymbol{p}}, \tilde{\alpha}^*)$$

where

$$\tilde{\alpha}^* = \tilde{\alpha}(\bar{\boldsymbol{p}}, \Delta_{\boldsymbol{p}}, \boldsymbol{d}^*, \boldsymbol{g})$$

and

$$\boldsymbol{d}^* = \underset{\boldsymbol{d}}{\operatorname{argmax}} \left\{ \tilde{\alpha}(\bar{\boldsymbol{p}}, \Delta_{\boldsymbol{p}}, \boldsymbol{d}, \boldsymbol{g}) \right\}.$$

When $\Delta_{\boldsymbol{p}}$, $\bar{\boldsymbol{p}}$, and $\boldsymbol{g}$ are understood from context, $\mathcal{M}(\Delta_{\boldsymbol{p}}, \bar{\boldsymbol{p}}, \boldsymbol{g})$ will be abbreviated as $\mathcal{M}$.

Solving for the optimal design requires identifying $\mathcal{M}$. Obviously, if $\mathcal{M}$ contains the support set $\Delta_{\boldsymbol{p}}$, the design is robust. In other words, the largest support set for which a robust design exists is given by $\mathcal{M}$. Note that if the solution to this problem is unique, the RDS corresponding to $\mathcal{M}$ is a singleton. Strategies for hyper-spherical and hyper-rectangular support sets are presented next. In the first one, called the P-Search, the support is the hyper-sphere $\mathcal{S}_{\boldsymbol{p}}(\bar{\boldsymbol{p}}, R)$. In the second one, called the Q-Search, the support is the hyper-rectangle $\mathcal{R}_{\boldsymbol{p}}(\bar{\boldsymbol{p}}, \boldsymbol{m})$. The uniqueness of the solution to the problem statement of interest cannot be guaranteed unless restrictions[5, 14] on the way in which $\boldsymbol{g}$ depends on $\boldsymbol{p}$ apply. More importantly, it may be possible to find designs whose CPV does not exist, i.e., designs for which $\mathcal{M}$ is unbounded. In these cases, where the constraints have no effect, the design is able to fully eliminate the dependence of the constraints on the uncertain parameter.

V..1. Hyper-Spheres

P-Search: If $\boldsymbol{g} \leq \boldsymbol{0}$ is a set of constraints and $\mathcal{S}_{\boldsymbol{p}}(\bar{\boldsymbol{p}}, R)$ is the support set, a design with the best robustness characteristics, namely $\boldsymbol{d}^{\mathcal{S}}$, and the corresponding $\mathcal{M}$ are given by

$$\boldsymbol{d}^{\mathcal{S}} = \underset{\boldsymbol{d}}{\operatorname{argmin}} \left\{ -\rho_{\mathcal{S}}(\bar{\boldsymbol{p}}, \tilde{\boldsymbol{p}}, \boldsymbol{d}) \right\}, \tag{27}$$

$$\mathcal{M} = \mathcal{S}_{\boldsymbol{p}} \left(\bar{\boldsymbol{p}}, \rho_{\mathcal{S}}(\bar{\boldsymbol{p}}, \tilde{\boldsymbol{p}}, \boldsymbol{d}^{\mathcal{S}}) \right). \tag{28}$$

A trivial example of the case in which th CPV does not exist is given by $\boldsymbol{g} = \boldsymbol{p}^T \boldsymbol{d} - 1$ and $\boldsymbol{d}^{\mathcal{S}} = \boldsymbol{0}$. This results in $\rho_{\mathcal{S}} = \infty$ and $\mathcal{M} = \mathbb{R}^{\dim(\boldsymbol{p})}$.

V..2. Hyper-Rectangles

Q-Search: If $\boldsymbol{g} \leq \mathbf{0}$ is a set of constraints and $\mathcal{R}_{\boldsymbol{p}}(\bar{\boldsymbol{p}}, \boldsymbol{m})$ is the support set, a design with the best robustness characteristics, namely $\boldsymbol{d}^{\mathcal{R}}$, and the corresponding $\mathcal{M}$ are given by

$$\boldsymbol{d}^{\mathcal{R}} = \underset{\boldsymbol{d}}{\text{argmin}} \left\{ -\rho_{\mathcal{R}}(\bar{\boldsymbol{p}}, \tilde{\boldsymbol{p}}, \boldsymbol{m}, \boldsymbol{d}) \right\}, \tag{29}$$

$$\mathcal{M} = \mathcal{R}_{\boldsymbol{p}} \left(\bar{\boldsymbol{p}}, \frac{\rho_{\mathcal{R}}(\bar{\boldsymbol{p}}, \tilde{\boldsymbol{p}}, \boldsymbol{m}, \boldsymbol{d}^{\mathcal{R}})}{\|\boldsymbol{m}\|} \boldsymbol{m} \right). \tag{30}$$

Note that $-\|\tilde{\boldsymbol{q}}\|$ can also be used as the objective of the optimization problem in Equation (29). Equation (30) is derived as follows. Let $\mathcal{S}_{\boldsymbol{q}}(\mathbf{0}, \|\tilde{\boldsymbol{q}}\|)$ be the hyper-sphere associated to $\boldsymbol{d}^{\mathcal{R}}$. According to Equation (19), $\hat{\boldsymbol{q}} = (\|\tilde{\boldsymbol{q}}\| \cdot \mathbf{1})/\sqrt{\dim(\boldsymbol{p})}$, on the surface of the hyper-sphere, corresponds to a vertex of a hyper-rectangle via $\hat{\boldsymbol{p}} = Q^{-1}(\hat{\boldsymbol{q}})$. Since $\hat{\boldsymbol{p}} = \rho_{\mathcal{R}} \boldsymbol{m}/\|\boldsymbol{m}\|$, $\mathcal{M} = \mathcal{R}_{\boldsymbol{p}}(\bar{\boldsymbol{p}}, \hat{\boldsymbol{p}})$.

V..3. RDS Existence

The results of the P- and Q-Searches can be used to determine if the RDS corresponding to a support with arbitrary shape exists. This is attained by using $\mathcal{M}$ as a reference.

Lemma 12 (RDS Existence). *Let $\Delta_{\boldsymbol{p}}$ have an arbitrary geometry. If $\Delta_{\boldsymbol{p}} \subseteq \mathcal{M}$, where $\mathcal{M}$ results from either Equation (28) or Equation (30), the RDS for the support set $\Delta_{\boldsymbol{p}}$ is non-empty. Conversely, if there exists a hyper-sphere $\mathcal{S}_{\boldsymbol{p}}(\bar{\boldsymbol{p}}, R) \subset \Delta_{\boldsymbol{p}}$ such that $R \geq \rho_{\mathcal{S}}(\bar{\boldsymbol{p}}, \tilde{\boldsymbol{p}}, \boldsymbol{d}^{\mathcal{S}})$, or if there exists a hyper-rectangle $\mathcal{R}_{\boldsymbol{p}}(\bar{\boldsymbol{p}}, \boldsymbol{m}) \subset \Delta_{\boldsymbol{p}}$ such that $\|\boldsymbol{m}\| > \rho_{\mathcal{R}}(\boldsymbol{p}, \boldsymbol{m}, \boldsymbol{d}^{\mathcal{R}})$, the RDS for the support set $\Delta_{\boldsymbol{p}}$ is empty.*

VI. Example

The analysis and design techniques presented in this paper are potentially applicable to a wide range of engineering problems. For instance, the parameterization of a model of a flexible structure includes modal frequencies and damping ratios which typically are only approximately known. In analyzing the dynamics of a spacecraft, there can be uncertainty in the designer's knowledge of the inertias and mass. In such cases, the constraint functions can be based on performance metrics. For purposes of illustration, however, some constraint functions will be given by mathematical formula with no underlying physical model assumed.

Several of the concepts proposed are illustrated hereafter. A problem which is two-dimensional in the design variables and in the uncertain parameter has been selected to facilitate visualization. Let the set of constraints be prescribed by

$$\boldsymbol{g} = \begin{bmatrix} 3\boldsymbol{d}_2 - 4\boldsymbol{p}_1^2 - 4\boldsymbol{d}_1\boldsymbol{p}_2 \sin\left(\boldsymbol{p}_2\boldsymbol{d}_1 - \boldsymbol{p}_1^2\right) \\ -\sin\left(\boldsymbol{p}_1^2\boldsymbol{p}_2 - \sin(2\boldsymbol{p}_1 - 2)\right) - \boldsymbol{d}_1\boldsymbol{d}_2\boldsymbol{p}_1 - \boldsymbol{p}_2 \\ \boldsymbol{d}_1 + \boldsymbol{p}_1^2\boldsymbol{d}_2^2 - 4\boldsymbol{p}_2^2\boldsymbol{p}_1 - 4\sin\left(2\boldsymbol{p}_1 - 2\boldsymbol{p}_2\right) \\ 2(\boldsymbol{p}_1 + \boldsymbol{p}_2)\sin(\boldsymbol{p}_1^2 - \boldsymbol{d}_2) - 2\boldsymbol{p}_1\boldsymbol{p}_2\left(\boldsymbol{d}_2 + 2\boldsymbol{p}_1^2 - 2\right) + \boldsymbol{d}_1 - 6\boldsymbol{p}_1 \end{bmatrix},$$

and the designated point be $\bar{\boldsymbol{p}} = [1, 1]^T$. The contour of the corresponding FDS, which (Definition 6) is independent of the choice of $\Delta_{\boldsymbol{p}}$, is marked with a solid thick line in subsequent figures.

This first illustration makes use of a spherical support set, $\Delta_{\boldsymbol{p}}$, centered at $\bar{\boldsymbol{p}}$. This choice of support set might indicate the analyst's judgment that the uncertainty in the uncertain parameter is geometrical in nature with no distinctions made based on the direction of perturbation from the designated point. For different design points in the FDS, the PSM $\rho_{\mathcal{S}}$ is calculated. As noted following Lemma 7, the PSM is independent of the radius of the spherical support set. Since by Definition 11 the PSM is determined by the CPV, the PSM is calculated by using Equations (15 - 18). The resulting PSMs are shown as a function of the design point $[\boldsymbol{d}_1, \boldsymbol{d}_2]^T$ in Figure 3. Recall that, for a given design point, its PSM is the size of the largest perturbation to $\bar{\boldsymbol{p}}$ allowed before a constraint might be violated. For ease of comparability, the color scale used in Figure 3 is the same as that in subsequent figures for rectangular PSMs. Figure 3 illustrates that the design with best robustness characteristics is able to tolerate uncertainty in $\boldsymbol{p} = \bar{\boldsymbol{p}} + \boldsymbol{u}$ with $\|\boldsymbol{u}\| \leq .53$. Therefore, variations of less than .53 lead to non-empty RDSs. The boundary of the FDS is given by the $\rho_{\mathcal{S}} = 0$ contour. Notice that multiple PSM maxima occur (there are local maxima in the vicinity of $[-1, 0]^T$ and of $[-2.2, -2.4]^T$). More importantly, notice that designs further in from the boundary of the FDS are not necessarily more robust. For instance, the comparison of $\boldsymbol{d}^{(1)} = [-2.25, -2.4]^T$ and $\boldsymbol{d}^{(2)} = [-1, -1]^T$ shows that $\rho_{\mathcal{S}}(\boldsymbol{d}^{(1)}) \gg \rho_{\mathcal{S}}(\boldsymbol{d}^{(2)})$ even though $\boldsymbol{d}^{(1)}$ is much closer to a constraint limiting the FDS than $\boldsymbol{d}^{(2)}$.

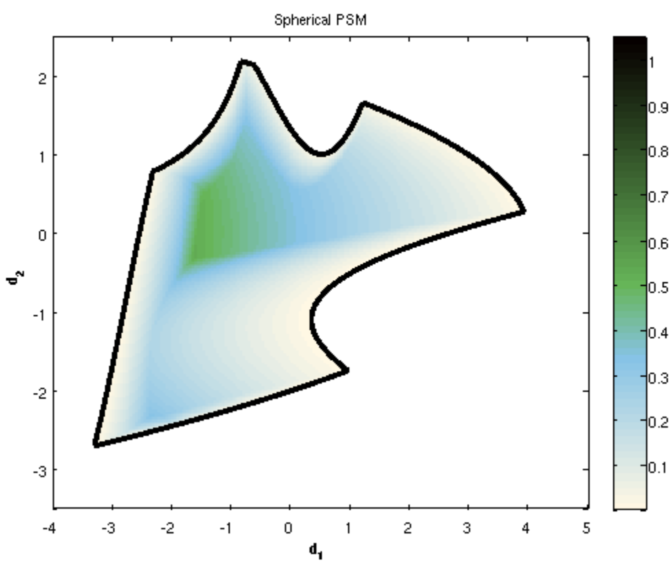

Figure 3. Spherical PSMs, $\rho_{\mathcal{S}}$, in the FDS.

Now we consider the rectangular support set $\Delta_{\boldsymbol{p}} = \mathcal{R}_{\boldsymbol{p}}(\bar{\boldsymbol{p}}, \boldsymbol{m}^{(1)})$ for $\boldsymbol{m}^{(1)} = [1, 1]^T$.

This choice of support set might indicate the analyst's judgment that the uncertainties in the components of the uncertain parameter are independent of each other, but of about the same magnitude. The corresponding rectangular-PSMs are shown in Figure 4. Larger margins are now attained than for the Spherical PSMs. Similarities in the distribution of PSMs arise since the offset between the circle, i.e., two-dimensional hyper-sphere, and the square, i.e., two dimensional regular hyper-rectangle, used is relatively small. Figure 5 shows the rectangular-PSM values for $\mathcal{R}_{\boldsymbol{p}}(\bar{\boldsymbol{p}}, \boldsymbol{m}^{(2)})$ where $\boldsymbol{m}^{(2)} = [1, 4]^T$. This choice of support set might indicate the analyst's judgment that the uncertainties in the components of the uncertain parameter are independent of each other, and that the level of uncertainty in the second component is about 4 times that of the first. Considerable differences in the distribution and magnitude of the PSMs, as compared to the previous two figures, are apparent. This indicates a strong dependence of the robustness on the geometry of the support set.

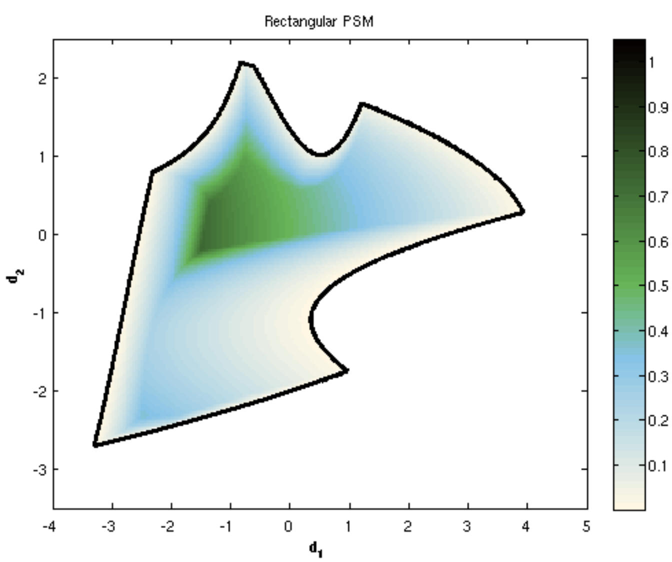

Figure 4. Rectangular PSMs, $\rho_{\mathcal{R}}$, for $\mathcal{R}(\bar{\boldsymbol{p}}, \boldsymbol{m}^{(1)})$.

An application of Bounding sets, as introduced in Section IV-IV.C, is now presented. Consider the triangular support set shown in the left of Figure 6 with a solid line. The tightest bounding circle and rectangle are superimposed. Clearly, the rectangle is a better approximation to the triangular support set. The RDSs corresponding to both bounding sets, calculated via spherical-PSMs and rectangular-PSMs, are shown in the right subplot of Figure 6. The RDS for the bounding circle is filled in with black while the RDS for the bounding rectangle is colored in dark gray. As expected, the RDS for the rectangle contains the RDS for the sphere. We have no such tools for the determination of the true RDS for the triangular support set, so we apply an approximation technique. For this, a probability

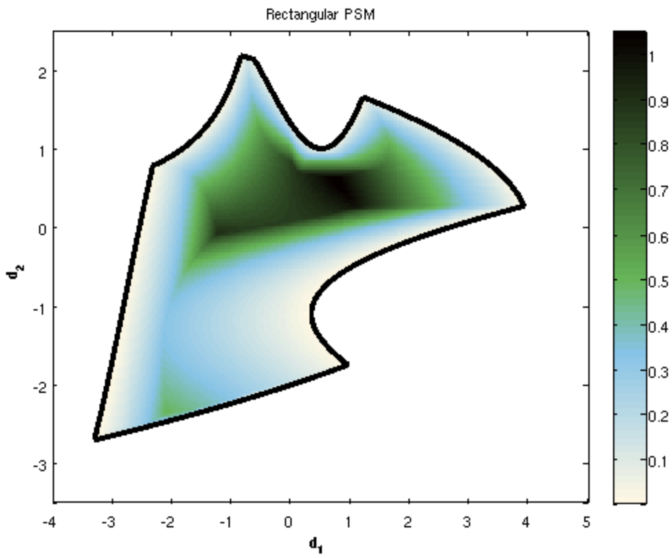

Figure 5. Rectangular PSMs, $\rho_{\mathcal{R}}$, for $\mathcal{R}(\bar{\boldsymbol{p}}, \boldsymbol{m}^{(2)})$.

density function having the triangle as the support set is assumed. By picking a fixed design point $\boldsymbol{d}$ and using a computationally intensive sampling procedure in $\boldsymbol{p}$-space, we can get a strong indication of whether or not $\boldsymbol{d}$ is in the RDS for the triangular support set. By repeating this for a sufficiently large number of design points, we obtain an approximation to the RDS. In a probabilistic model, the RDS is characterized by $P[\mathcal{F}(\boldsymbol{d}, \boldsymbol{g})] = 0$. In theory, this approximation depends on the support set only, not on the probability density function assumed. In practice, this is not the case due to the numerical error caused by using a sample set of finite size. The corresponding RDS is colored with light gray. The approximations to the RDS for the triangular support set resulting from using the bounding sets are both subsets of the sampling based approximation, $\{d : P[\mathcal{F}(\boldsymbol{d}, \boldsymbol{g})] = 0\}$, to the RDS. The conservatism introduced by using the bounding circle leads to a considerably smaller RDS approximation. Note that the portion of the RDS in the vicinity of $\boldsymbol{d} = [-2, -2.25]^T$ is completely omitted by the approximation based on the circular bounding set. Obviously, the RDS corresponding to the rectangle is a better approximation since the offset between the rectangle and the triangle is smaller. As expected, bounding of the uncertainty set introduces conservatism by artificially reducing the design space available. This conservatism might lead to an empty approximation of the RDS, even though the actual RDS is non-empty. Notice however, that while the $P[\mathcal{F}] = 0$ contour is the best approximation to the boundary of the RDS shown, only the iso-PSM contours resulting from bounding provide a formal guarantee of the existence of the RDS. Recall that when the support set is a hyper-sphere or a hyper-rectangle, the actual RDS, providing it exists, can be calculated exactly using PSMs. In such a case, the $P[\mathcal{F}] = 0$ and an iso-PSM contours coincide.

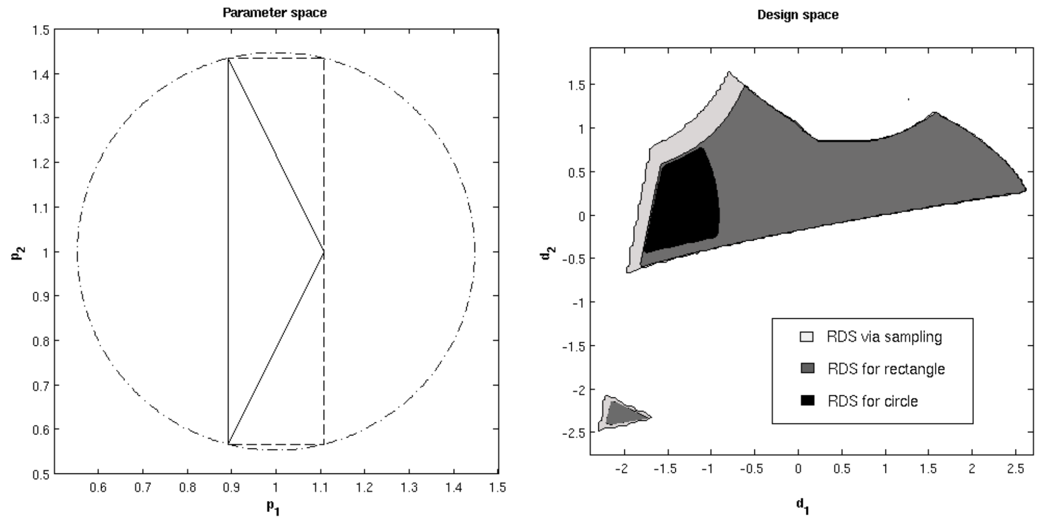

Figure 6. Left: triangular support and two bounding sets. Right: corresponding RDS approximations.

A robust design of Section V is generated next. While the search for the design with best robustness characteristics corresponding to a circular support leads to $\boldsymbol{d}^{\mathcal{S}} = [-1.65, -0.33]^T$ and $\mathcal{M} = \mathcal{S}_{\boldsymbol{p}}(\bar{\boldsymbol{p}}, 0.53)$, the one corresponding to the rectangular support set $\mathcal{R}_{\boldsymbol{p}}(\bar{\boldsymbol{p}}, \boldsymbol{m}^{(2)})$ leads to $\boldsymbol{d}^{\mathcal{R}} = [0.718, 0.631]^T$ and $\mathcal{M} = \mathcal{R}_{\boldsymbol{p}}(\bar{\boldsymbol{p}}, 0.26\boldsymbol{m}^{(2)})$. These sets are shown in Figures 7 and 8 along with the corresponding CPVs. Note that changing the design point has altered the constraint boundaries. Three CPVs exist in both cases. Recall that support sets proportional and larger than $\mathcal{M}$ lead to an empty RDS.

VII. Concluding Remarks

A methodology for robustness analysis and robust-design of systems subject to parametric uncertainty is proposed herein. Emphasis is given to uncertainty sets prescribed (or bounded) by hyper-spheres or hyper-rectangles since such sets are commonly used in engineering applications. Formal assessments of robustness are possible since these sets admit a rigorous mathematical manipulation. The robustness tests proposed should precede studies based on the propagation of probabilistic uncertainty models. Failure to do so might lead to inefficient numerical implementations. The efficient inclusion of hard inequality constraints into design optimization schemes is made possible because the sampling/partitioning of the parameter space is avoided. Many of the developments proposed extend the state of the art on the subject matter. The scope of the ideas proposed is generic, making them applicable to a broad spectrum of engineering problems and disciplines.

There are several directions which future research could take. For example, more freedom could be given to the geometry of the uncertainty model such as more general shapes for the

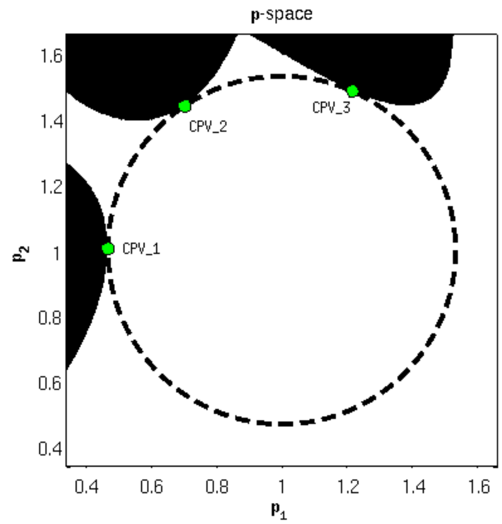

Figure 7. $\mathcal{M}$ for a circular support.

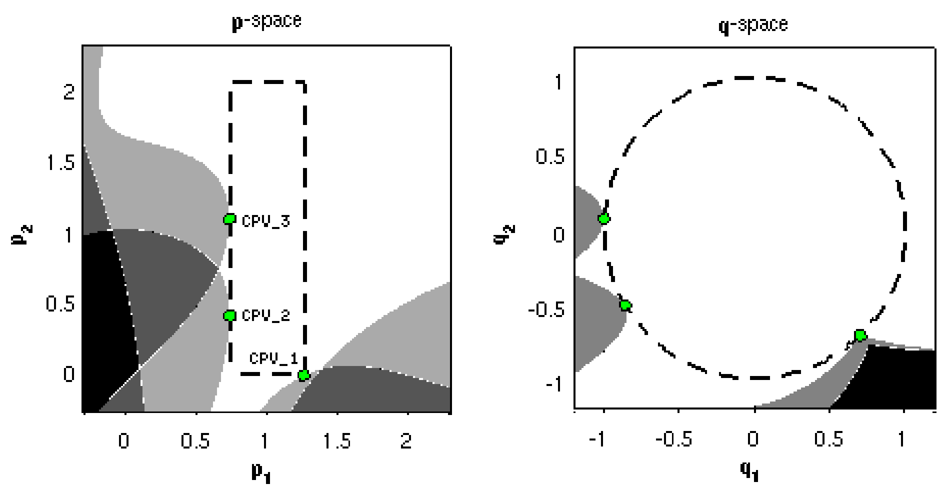

Figure 8. Left: $\mathcal{M}$ proportional to $\mathcal{R}(\bar{p}, m^{(2)})$. Right: corresponding set in q-space.

support set and/or non-central placement of the designated point. Also, the uncertain parameters could be assigned probability distributions, and the geometric techniques presented here could be applied to the problem of estimating probability of failure.

VIII. Appendix

Proof of Lemma 1. Since the components of $\boldsymbol{g}$ are continuous, each $\mathcal{F}_i$ is an open set, and therefore $\mathcal{F}$ is also. Thus, $\boldsymbol{p} \in \partial\mathcal{F}$ implies that $\boldsymbol{p} \notin \mathcal{F}$; so $\boldsymbol{g}_i(\boldsymbol{p}, \boldsymbol{d}) \leq 0$ for all i. On the other hand, $\boldsymbol{p} \in \partial\mathcal{F}$ implies that there is a sequence of points $\{\boldsymbol{p}^{(n)}\} \subset \mathcal{F}$ such that $\lim_{n\to\infty} \boldsymbol{p}^{(n)} = \boldsymbol{p}$. By taking a subsequence and renaming it $\{\boldsymbol{p}^{(n)}\}$, we may assume that there is some i for which all $\boldsymbol{p}^{(n)} \in \mathcal{F}_i$. This means that $\boldsymbol{g}_i(\boldsymbol{p}^{(n)}, \boldsymbol{d}) > 0$ for all n, so, again by continuity, $\boldsymbol{g}_i(\boldsymbol{p}, \boldsymbol{d}) = \lim_{n\to\infty} \boldsymbol{g}_i(\boldsymbol{p}^{(n)}, \boldsymbol{d}) \geq 0$. This shows that there is an i for which $\boldsymbol{g}_i(\boldsymbol{p}, \boldsymbol{d}) = 0$. □

Proof of Lemma 2. Conclusion (a): It must be shown that for some $\hat{\alpha} > 0$, no point of the interval $[0, \hat{\alpha})$ touches $\tilde{A}$. Using the hypotheses (ii) and (v) it follows that there is a *neighborhood* of $\bar{\boldsymbol{p}}$ which contains no constraint violations. (A *neighborhood* of $\bar{\boldsymbol{p}}$ is a set of the form $\{\boldsymbol{p} : \|\boldsymbol{p} - \bar{\boldsymbol{p}}\| < \delta\}$ for some positive value of δ.) But, using the boundedness from hypothesis (i), it follows that for all sufficiently small α, there are no constraint violations in $\mathcal{H}(\Delta_{\boldsymbol{p}}, \bar{\boldsymbol{p}}, \alpha)$.

Conclusion (b): Since (hypothesis iii) $\bar{\boldsymbol{p}}$ is interior to $\Delta_{\boldsymbol{p}}$, $\Delta_{\boldsymbol{p}}$ contains a ball of positive radius centered at $\bar{\boldsymbol{p}}$. Thus, any point in $\mathbb{R}^{\dim(\boldsymbol{p})}$ is covered by $\mathcal{H}(\Delta_{\boldsymbol{p}}, \bar{\boldsymbol{p}}, \alpha)$ for sufficiently large α. Since (hypothesis iv) $\mathcal{F}$ is not empty, $\tilde{A}$ is not empty, and conclusion (b) follows.

Conclusion (c): Since (hypothesis ii) the constraint functions are continuous, and the constraint violation set $\mathcal{F}$ is defined by strict positivity of one of the component constraint functions, it follows that, whenever a positive α is in $\tilde{A}$, there is also a smaller α' which is also in $\tilde{A}$. Thus, if the infimum of $\tilde{A}$ is positive, it cannot be a member of $\tilde{A}$. Conclusion (c) follows.

Conclusion (d) is established by constructing a point $\tilde{\boldsymbol{p}}$ which is then proven to be a member of both $\partial\mathcal{H}(\Delta_{\boldsymbol{p}}, \bar{\boldsymbol{p}}, \tilde{\alpha})$ and $\partial\mathcal{F}$. By definition of $\tilde{\alpha}$ and since $\tilde{\alpha} < \infty$, there must be a sequence $\alpha^{(n)} \downarrow \tilde{\alpha}$ such that $\mathcal{H}(\Delta_{\boldsymbol{p}}, \bar{\boldsymbol{p}}, \alpha^{(n)}) \cap \mathcal{F} \neq \emptyset$. Pick $\boldsymbol{p}^{(n)} \in \mathcal{H}(\Delta_{\boldsymbol{p}}, \bar{\boldsymbol{p}}, \alpha^{(n)}) \cap \mathcal{F}$. For each n, there must be an i for which $\boldsymbol{g}_i(\boldsymbol{p}^{(n)}, \boldsymbol{d}) > 0$. Since there are only finitely many possible values of i, a subsequence of $\{\boldsymbol{p}^{(n)}\}$ may be extracted, and $\{\boldsymbol{p}^{(n)}\}$ and $\{\alpha^{(n)}\}$ will now refer to that subsequence and the corresponding α subsequence, for which there is a single i that makes $\boldsymbol{g}_i(\boldsymbol{p}^{(n)}, \boldsymbol{d}) > 0$ for all n. Now, since $\{\boldsymbol{p}^{(n)}\} \in \mathcal{H}(\Delta_{\boldsymbol{p}}, \bar{\boldsymbol{p}}, \alpha^{(n)})$, there must exist a $\boldsymbol{q}^{(n)} \in \Delta_{\boldsymbol{p}}$ such that $\boldsymbol{p}^{(n)} = \alpha^{(n)}(\boldsymbol{q}^{(n)} - \bar{\boldsymbol{p}}) + \bar{\boldsymbol{p}}$. Rewrite this equation as

$$\boldsymbol{p}^{(n)} = \tilde{\alpha}(\boldsymbol{q}^{(n)} - \bar{\boldsymbol{p}}) + \bar{\boldsymbol{p}} + (\alpha^{(n)} - \tilde{\alpha})(\boldsymbol{q}^{(n)} - \bar{\boldsymbol{p}}). \tag{31}$$

Since $\boldsymbol{q}^{(n)} \in \Delta_{\boldsymbol{p}}$, a compact set, some subsequence of the $\boldsymbol{q}$ sequence converges, say to $\tilde{\boldsymbol{q}}$. Once again, rename things so that $\{\boldsymbol{q}^{(n)}\}$ now refers to this subsequence and $\{\boldsymbol{p}^{(n)}\}$ and $\{\alpha^{(n)}\}$ are the corresponding subsequences. Then the first term on the right hand side of Equation (31) converges to $\tilde{\alpha}(\tilde{\boldsymbol{q}} - \bar{\boldsymbol{p}})$ and the third term converges to zero. Thus, $\boldsymbol{p}^{(n)}$ converges. Call the limit $\tilde{\boldsymbol{p}}$. It follows that

$$\tilde{\boldsymbol{p}} = \tilde{\alpha}(\tilde{\boldsymbol{q}} - \bar{\boldsymbol{p}}) + \bar{\boldsymbol{p}} \in \mathcal{H}(\Delta_{\boldsymbol{p}}, \bar{\boldsymbol{p}}, \tilde{\alpha}).$$

Recall that points on the boundary of a set are characterized by the property that each ball of positive radius, no matter how small, which is centered at such a point intersects both the set and its complement. Each such ball is called a *neighborhood* of the point. Since $\tilde{\boldsymbol{p}} \in \mathcal{H}(\Delta_{\boldsymbol{p}}, \bar{\boldsymbol{p}}, \tilde{\alpha})$, each neighborhood of $\tilde{\boldsymbol{p}}$ intersects both $\mathcal{H}(\Delta_{\boldsymbol{p}}, \bar{\boldsymbol{p}}, \tilde{\alpha})$ and, since conclusion (c) holds under the present hypotheses, the complement of $\mathcal{F}$. Also, each neighborhood of $\tilde{\boldsymbol{p}}$ contains some $\boldsymbol{p}^{(n)}$, and so intersects both $\mathcal{F}$ and, again by conclusion (c), the complement of $\mathcal{H}(\Delta_{\boldsymbol{p}}, \bar{\boldsymbol{p}}, \tilde{\alpha})$. This shows that $\tilde{\boldsymbol{p}}$ is in both $\partial\mathcal{H}(\Delta_{\boldsymbol{p}}, \bar{\boldsymbol{p}}, \tilde{\alpha})$ and $\partial\mathcal{F}$.

□

Proof of Lemma 3. "If": Suppose $\Delta_{\boldsymbol{p}}$ is star convex with respect to $\bar{\boldsymbol{p}}$, $0 \le \alpha_1 < \alpha_2$, and $\boldsymbol{p} \in \mathcal{H}(\Delta_{\boldsymbol{p}}, \bar{\boldsymbol{p}}, \alpha_1)$. Then for some $\boldsymbol{q} \in \Delta_{\boldsymbol{p}}$, $\boldsymbol{p} = \alpha_1(\boldsymbol{q} - \bar{\boldsymbol{p}}) + \bar{\boldsymbol{p}}$. But then

$$\boldsymbol{p} = \alpha_2 \left[\frac{\alpha_1}{\alpha_2}\boldsymbol{q} + \left(1 - \frac{\alpha_1}{\alpha_2}\right)\bar{\boldsymbol{p}} \right] + \bar{\boldsymbol{p}} \in \mathcal{H}(\Delta_{\boldsymbol{p}}, \bar{\boldsymbol{p}}, \alpha_2),$$

since the bracketed quantity is a convex combination of $\boldsymbol{q}$ and $\bar{\boldsymbol{p}}$ and so, by star convexity, is in $\Delta_{\boldsymbol{p}}$.

"Only if": Suppose $\Delta_{\boldsymbol{p}}$ is not star convex with respect to $\bar{\boldsymbol{p}}$. Then for some $\boldsymbol{p} \in \Delta_{\boldsymbol{p}}$ and some α with $0 \le \alpha < 1$, $\boldsymbol{q} \triangleq \alpha\boldsymbol{p} + (1-\alpha)\bar{\boldsymbol{p}} \notin \Delta_{\boldsymbol{p}}$. But, $\boldsymbol{q} = \alpha(\boldsymbol{p} - \bar{\boldsymbol{p}}) + \bar{\boldsymbol{p}} \in \mathcal{H}(\Delta_{\boldsymbol{p}}, \bar{\boldsymbol{p}}, \alpha)$. This implies that $\mathcal{H}(\Delta_{\boldsymbol{p}}, \bar{\boldsymbol{p}}, \alpha) \not\subset \mathcal{H}(\Delta_{\boldsymbol{p}}, \bar{\boldsymbol{p}}, 1)$ contradicting the homothetic monotonicity of the uncertainty model $\langle \Delta_{\boldsymbol{p}}, \bar{\boldsymbol{p}} \rangle$. □

Proof of Lemma 4. "Only if": Suppose $\boldsymbol{d}$ is a robust design. Then $\Delta_{\boldsymbol{p}} \cap \mathcal{F} = \emptyset$. Since $\Delta_{\boldsymbol{p}} = \mathcal{H}(\Delta_{\boldsymbol{p}}, \bar{\boldsymbol{p}}, 1)$ and $\langle \Delta_{\boldsymbol{p}}, \bar{\boldsymbol{p}} \rangle$ is homotheticly monotone, $[0, 1] \cap \tilde{A} = \emptyset$. Thus, $\tilde{\alpha} \ge 1$.

"If": It will be shown that if $\boldsymbol{d}$ is not a robust design, $\tilde{\alpha} < 1$. But, if $\boldsymbol{d}$ is not a robust design, $\Delta_{\boldsymbol{p}} \cap \mathcal{F} \ne \emptyset$. Let $\boldsymbol{p}$ be an element of this intersection. Then $\boldsymbol{p}^{(\alpha)} \triangleq \alpha(\boldsymbol{p} - \bar{\boldsymbol{p}}) + \bar{\boldsymbol{p}} \in \mathcal{H}(\Delta_{\boldsymbol{p}}, \bar{\boldsymbol{p}}, \alpha)$. Now, $\boldsymbol{p} - \boldsymbol{p}^{(\alpha)} = (1-\alpha)(\boldsymbol{p} - \bar{\boldsymbol{p}})$, so $\boldsymbol{p}^{(\alpha)}$ can be placed arbitrarily close to $\boldsymbol{p}$ by choosing α close enough to 1. Since $\mathcal{F}$ is an open set, a choice of $\alpha < 1$ can be made so that $\boldsymbol{p}^{(\alpha)} \in \mathcal{F}$. For this α, $\mathcal{H}(\Delta_{\boldsymbol{p}}, \bar{\boldsymbol{p}}, \alpha) \cap \mathcal{F} \ne \emptyset$. Therefore, $\alpha \in \tilde{A}$, so $\tilde{\alpha} \le \alpha < 1$. □

Proof of Lemma 5. Under the present hypotheses, Lemma 2(d) may be applied. Thus, there is a $\tilde{\boldsymbol{p}} \in \partial\mathcal{H}(\Delta_{\boldsymbol{p}}, \bar{\boldsymbol{p}}, \tilde{\alpha}) \cap \partial\mathcal{F}$. Since $\Delta_{\boldsymbol{p}}$ is compact, it follows that $\mathcal{H}(\Delta_{\boldsymbol{p}}, \bar{\boldsymbol{p}}, \alpha)$ are compact for all α. Therefore,

$$\partial\mathcal{H}(\Delta_{\boldsymbol{p}}, \bar{\boldsymbol{p}}, \alpha) \subset \mathcal{H}(\Delta_{\boldsymbol{p}}, \bar{\boldsymbol{p}}, \alpha).$$

Also, since $\mathcal{F} = \cup_{k=1}^{\dim(\boldsymbol{g})} \mathcal{F}_k$, and these are all open sets, it follows that

$$\overline{\mathcal{F}_k} \subset \overline{\mathcal{F}}, \quad \partial\mathcal{F} \subset \bigcup_{k=1}^{\dim(\boldsymbol{g})} \partial\mathcal{F}_k \subset \overline{\mathcal{F}} \quad \text{and} \quad \partial\mathcal{F}_k \subset \bigcup_{k=1}^{\dim(\boldsymbol{g})} \partial\mathcal{F}_k \subset \overline{\mathcal{F}} \text{ for all } k.$$

Recall that the definition of $\tilde{\alpha}$ can be written

$$\tilde{\alpha} \triangleq \inf \left\{ \alpha : \mathcal{H}(\Delta_{\boldsymbol{p}}, \bar{\boldsymbol{p}}, \alpha) \bigcap \mathcal{F} \ne \emptyset \right\}.$$

Make the definitions

$$
\begin{aligned}
\hat{\alpha} &\triangleq \inf\left\{\alpha : \mathcal{H}(\Delta_{\boldsymbol{p}}, \bar{\boldsymbol{p}}, \alpha) \bigcap \overline{\mathcal{F}} \neq \emptyset\right\}, \\
\alpha' &\triangleq \inf\left\{\alpha : \partial\mathcal{H}(\Delta_{\boldsymbol{p}}, \bar{\boldsymbol{p}}, \alpha) \bigcap \left[\bigcup_{k=1}^{\dim(\boldsymbol{g})} \partial\mathcal{F}_k\right] \neq \emptyset\right\}, \\
\alpha'' &\triangleq \min\left\{\alpha_1, \alpha_2, \cdots, \alpha_{\dim(\boldsymbol{g})}\right\}, \text{ where} \\
&\quad \alpha_k \triangleq \inf\left\{\alpha : \partial\mathcal{H}(\Delta_{\boldsymbol{p}}, \bar{\boldsymbol{p}}, \alpha) \bigcap \partial\mathcal{F}_k \neq \emptyset\right\} \text{ for } 1 \leq k \leq \dim(\boldsymbol{g}), \text{ and} \\
\bar{\alpha} &\triangleq \min\left\{\bar{\alpha}_1, \bar{\alpha}_2, \cdots, \bar{\alpha}_{\dim(\boldsymbol{g})}\right\}, \text{ where} \\
&\quad \bar{\alpha}_k \triangleq \inf\left\{\alpha : \partial\mathcal{H}(\Delta_{\boldsymbol{p}}, \bar{\boldsymbol{p}}, \alpha) \bigcap \overline{\mathcal{F}_k} \neq \emptyset\right\} \text{ for } 1 \leq k \leq \dim(\boldsymbol{g}).
\end{aligned}
$$

One by one, the inequalities

$$
\hat{\alpha} \leq \alpha', \quad \alpha' \leq \alpha'', \quad \hat{\alpha} \leq \bar{\alpha}, \quad \bar{\alpha} \leq \alpha'', \quad \alpha'' \leq \tilde{\alpha}, \quad \text{and} \quad \tilde{\alpha} \leq \hat{\alpha}
$$

will be established, showing that all these αs are equal.

$\hat{\alpha} \leq \alpha'$: The set inclusions stated at the beginning of this proof imply that, for all α,

$$
\partial\mathcal{H}(\Delta_{\boldsymbol{p}}, \bar{\boldsymbol{p}}, \alpha) \bigcap \left[\bigcup_{k=1}^{\dim(\boldsymbol{g})} \partial\mathcal{F}_k\right] \subset \mathcal{H}(\Delta_{\boldsymbol{p}}, \bar{\boldsymbol{p}}, \alpha) \bigcap \overline{\mathcal{F}}.
$$

It follows that

$$
\left\{\alpha : \partial\mathcal{H}(\Delta_{\boldsymbol{p}}, \bar{\boldsymbol{p}}, \alpha) \bigcap \left[\bigcup_{k=1}^{\dim(\boldsymbol{g})} \partial\mathcal{F}_k\right] \neq \emptyset\right\} \subset \left\{\alpha : \mathcal{H}(\Delta_{\boldsymbol{p}}, \bar{\boldsymbol{p}}, \alpha) \bigcap \overline{\mathcal{F}} \neq \emptyset\right\}.
$$

The inequality $\hat{\alpha} \leq \alpha'$ is an immediate consequence.

$\alpha' \leq \alpha''$: A similar argument based on which sets are subsets of which other sets yields the result that, for each k, $\alpha' \leq \alpha_k$. It follows immediately that $\alpha' \leq \alpha''$.

$\hat{\alpha} \leq \bar{\alpha}$: Similarly, $\hat{\alpha} \leq \bar{\alpha}_k$ for each k, so $\hat{\alpha} \leq \bar{\alpha}$.

$\bar{\alpha} \leq \alpha''$: Similarly, $\alpha_k \leq \bar{\alpha}_k$ for each k, so $\bar{\alpha} \leq \alpha''$.

$\alpha'' \leq \tilde{\alpha}$: Under the present hypotheses, Lemma 2(d) holds. Thus, there exists a point $\tilde{\boldsymbol{p}} \in \partial\mathcal{H}(\Delta_{\boldsymbol{p}}, \bar{\boldsymbol{p}}, \tilde{\alpha}) \cap \partial\mathcal{F}$. Then, for some k, $\tilde{\boldsymbol{p}} \in \partial\mathcal{H}(\Delta_{\boldsymbol{p}}, \bar{\boldsymbol{p}}, \tilde{\alpha}) \cap \partial\mathcal{F}_k$. Therefore, $\alpha_k \leq \tilde{\alpha}$. It follows that $\alpha'' \leq \tilde{\alpha}$.

$\tilde{\alpha} \leq \hat{\alpha}$: This is true if, for every α for which $\mathcal{H}(\Delta_{\boldsymbol{p}}, \bar{\boldsymbol{p}}, \alpha) \bigcap \overline{\mathcal{F}} \neq \emptyset$, it is also true that $\tilde{\alpha} \leq \alpha$. Fix such an α and let $\boldsymbol{p} \in \mathcal{H}(\Delta_{\boldsymbol{p}}, \bar{\boldsymbol{p}}, \alpha) \bigcap \overline{\mathcal{F}}$. If $\boldsymbol{p} \in \mathcal{F}$, then $\tilde{\alpha} \leq \alpha$. So, suppose $\boldsymbol{p} \in \partial\mathcal{F}$. We will show that $\tilde{\alpha} \leq \alpha$ by showing that, for every $\alpha^\circ > \alpha$, $\tilde{\alpha} \leq \alpha^\circ$. So, fix $\alpha^\circ > \alpha$. To show that $\tilde{\alpha} \leq \alpha^\circ$, we need to show that $\mathcal{H}(\Delta_{\boldsymbol{p}}, \bar{\boldsymbol{p}}, \alpha^\circ) \cap \mathcal{F} \neq \emptyset$.

Now, since $\boldsymbol{p} \in \mathcal{H}(\Delta_{\boldsymbol{p}}, \bar{\boldsymbol{p}}, \alpha)$, there is a $\boldsymbol{q} \in \Delta_{\boldsymbol{p}}$ for which

$$\boldsymbol{p} = \alpha(\boldsymbol{q} - \bar{\boldsymbol{p}}) + \bar{\boldsymbol{p}}.$$

Set

$$\boldsymbol{r} = \frac{\alpha}{\alpha^\circ}\boldsymbol{q} + (1 - \frac{\alpha}{\alpha^\circ})\bar{\boldsymbol{p}}.$$

Then

$$\boldsymbol{p} = \alpha^\circ(\boldsymbol{r} - \bar{\boldsymbol{p}}) + \bar{\boldsymbol{p}} \in \mathcal{H}(\Delta_{\boldsymbol{p}}, \bar{\boldsymbol{p}}, \alpha^\circ).$$

Since $\alpha < \alpha^\circ$, either $\boldsymbol{r}$ is an interior point of the line segment joining $\bar{\boldsymbol{p}}$ and $\boldsymbol{q}$, in which case $\boldsymbol{r}$ is an interior point of $\Delta_{\boldsymbol{p}}$ by strict star convexity of $\Delta_{\boldsymbol{p}}$ with respect to $\bar{\boldsymbol{p}}$, or $\boldsymbol{r} = \bar{\boldsymbol{p}}$, in which case $\boldsymbol{r}$ is an interior point of $\Delta_{\boldsymbol{p}}$ by hypothesis. In either case, there is a neighborhood $N_{\boldsymbol{r}}$ of $\boldsymbol{r}$ which is a subset of $\Delta_{\boldsymbol{p}}$. Then,

$$N_{\boldsymbol{p}} \triangleq \alpha^\circ(N_{\boldsymbol{r}} - \bar{\boldsymbol{p}}) + \bar{\boldsymbol{p}}$$

is a neighborhood of $\boldsymbol{p}$ which is a subset of $\mathcal{H}(\Delta_{\boldsymbol{p}}, \bar{\boldsymbol{p}}, \alpha^\circ)$. Since $\boldsymbol{p} \in \partial\mathcal{F}$, it follows that $\mathcal{H}(\Delta_{\boldsymbol{p}}, \bar{\boldsymbol{p}}, \alpha^\circ) \cap \mathcal{F} \neq \emptyset$. This shows that $\tilde{\alpha} \leq \alpha^\circ$ which was what was needed to complete the proof that $\tilde{\alpha} \leq \hat{\alpha}$.

We now know that $\tilde{\alpha} = \hat{\alpha} = \alpha' = \alpha'' = \bar{\alpha}$. Since the point $\tilde{\boldsymbol{p}}$ introduced earlier in this proof is in both the sets $\mathcal{H}(\Delta_{\boldsymbol{p}}, \bar{\boldsymbol{p}}, \alpha) \cap \overline{\mathcal{F}}$ and $\partial\mathcal{H}(\Delta_{\boldsymbol{p}}, \bar{\boldsymbol{p}}, \alpha) \cap \left[\cup_{k=1}^{\dim(\boldsymbol{g})} \partial\mathcal{F}_k\right]$, $\tilde{\alpha}$ is an element of the sets whose *infima* define $\hat{\alpha}$ and α'. So, in those definitions, "inf" can be replaced by "min." Since everything which has been proven so far can be applied to the case that the set of constraint functions $\boldsymbol{g}$ contains the single function $\boldsymbol{g}_k$, the "inf" in each of the definitions of α'' and $\bar{\alpha}$ can also be replaced by "min." This completes the proof of this Lemma.

□

Proof of Lemma 6. As noted in the Remark following the statement of this Lemma, it is the burden of Lemma 5 that these minima all produce $\tilde{\alpha}$ as an answer. What needs to be proven is that any $\boldsymbol{p}$ value in the sets corresponding to $\alpha = \tilde{\alpha}$ in the "constraint" portion of the optimization problem statements in Equations (10) - (13) is actually a CPV; i.e., is in $\partial\mathcal{H}(\Delta_{\boldsymbol{p}}, \bar{\boldsymbol{p}}, \tilde{\alpha}) \cap \partial\mathcal{F}$. E.g., to establish the characterization (10), it must be shown that if $\boldsymbol{p} \in \mathcal{H}(\Delta_{\boldsymbol{p}}, \bar{\boldsymbol{p}}, \tilde{\alpha}) \bigcap \overline{\mathcal{F}}$ then $\boldsymbol{p} \in \partial\mathcal{H}(\Delta_{\boldsymbol{p}}, \bar{\boldsymbol{p}}, \tilde{\alpha}) \cap \partial\mathcal{F}$, thus satisfying the definition of a CPV (Definition (5)).

Proof of (10): Let $\hat{\boldsymbol{p}} \in \mathcal{H}(\Delta_{\boldsymbol{p}}, \bar{\boldsymbol{p}}, \tilde{\alpha}) \bigcap \overline{\mathcal{F}}$. It is first shown that $\hat{\boldsymbol{p}} \in \partial\mathcal{F}$. Suppose the contrary. Then $\hat{\boldsymbol{p}} \in \mathcal{F}$. Since $\mathcal{F}$ is an open set, there is some neighborhood $N_{\hat{\boldsymbol{p}}}$ of $\hat{\boldsymbol{p}}$ which is a subset of $\mathcal{F}$. Thus, the line segment from $\bar{\boldsymbol{p}}$ to $\hat{\boldsymbol{p}}$ intersects $N_{\hat{\boldsymbol{p}}}$ and, therefore $\mathcal{F}$ not only at $\hat{\boldsymbol{p}}$, but at additional points closer to $\bar{\boldsymbol{p}}$ than $\hat{\boldsymbol{p}}$. Let $\boldsymbol{p}'$ be one such point. Then both $\boldsymbol{p}' \in \mathcal{F}$ and $\boldsymbol{p}' \in \mathcal{H}(\Delta_{\boldsymbol{p}}, \bar{\boldsymbol{p}}, \alpha')$ for some $\alpha' < \tilde{\alpha}$. This last membership is a consequence of $\boldsymbol{p}'$ being on the line segment joining $\bar{\boldsymbol{p}}$ and $\hat{\boldsymbol{p}}$, and being closer to $\bar{\boldsymbol{p}}$ than $\hat{\boldsymbol{p}}$, together with the star convexity of $\Delta_{\boldsymbol{p}}$ with respect to $\bar{\boldsymbol{p}}$. This contradicts the defining property of $\tilde{\alpha}$ which shows that $\hat{\boldsymbol{p}}$ must have been in $\partial\mathcal{F}$ in the first place. Now suppose that $\hat{\boldsymbol{p}} \notin \partial\mathcal{H}(\Delta_{\boldsymbol{p}}, \bar{\boldsymbol{p}}, \tilde{\alpha})$.

Then some neighborhood $N_{\hat{\boldsymbol{p}}}$ of $\hat{\boldsymbol{p}}$ is a subset of $\mathcal{H}(\Delta_{\boldsymbol{p}}, \bar{\boldsymbol{p}}, \tilde{\alpha})$. Since it has just been shown that $\hat{\boldsymbol{p}} \in \partial\mathcal{F}$, $N_{\hat{\boldsymbol{p}}}$ intersects $\mathcal{F}$, i.e., there is a point $\boldsymbol{p}'$ which is an interior point of both $\mathcal{F}$ (since all of its points are interior points) and of $\mathcal{H}(\Delta_{\boldsymbol{p}}, \bar{\boldsymbol{p}}, \tilde{\alpha})$ (since $\boldsymbol{p}'$ is in the open subset $N_{\hat{\boldsymbol{p}}}$ of $\mathcal{H}(\Delta_{\boldsymbol{p}}, \bar{\boldsymbol{p}}, \tilde{\alpha})$. But this means that we can move a small positive distance along the line segment from $\boldsymbol{p}'$ to $\bar{\boldsymbol{p}}$ without leaving either $\mathcal{F}$ or $\mathcal{H}(\Delta_{\boldsymbol{p}}, \bar{\boldsymbol{p}}, \tilde{\alpha})$. But, by doing this, just as before we find a point which is in both $\mathcal{F}$ and $\mathcal{H}(\Delta_{\boldsymbol{p}}, \bar{\boldsymbol{p}}, \alpha')$ for some $\alpha' < \tilde{\alpha}$. Once again, this contradicts the defining property of $\tilde{\alpha}$ which shows that $\hat{\boldsymbol{p}}$ must also have been in $\partial\mathcal{H}(\Delta_{\boldsymbol{p}}, \bar{\boldsymbol{p}}, \tilde{\alpha})$. This completes demonstrating (10).

Proof of (11): This is immediate from (10) since $\partial\mathcal{H}(\Delta_{\boldsymbol{p}}, \bar{\boldsymbol{p}}, \alpha) \bigcap \partial\mathcal{F} \subset \mathcal{H}(\Delta_{\boldsymbol{p}}, \bar{\boldsymbol{p}}, \alpha) \bigcap \overline{\mathcal{F}}$.

Proof of (12): Since (Lemma 5, Equation(8)) $\tilde{\alpha}_n = \tilde{\alpha}$,

$$\tilde{\boldsymbol{p}}^{(n)} \in \partial\mathcal{H}(\Delta_{\boldsymbol{p}}, \bar{\boldsymbol{p}}, \tilde{\alpha}) \bigcap \partial\mathcal{F}_n \subset \partial\mathcal{H}(\Delta_{\boldsymbol{p}}, \bar{\boldsymbol{p}}, \tilde{\alpha}) \bigcap \left[\bigcup_{k=1}^{\dim(\boldsymbol{g})} \partial\mathcal{F}_k \right].$$

Thus, by (11), $\tilde{\boldsymbol{p}}^{(n)}$ is a CPV.

Proof of (13): By repeating the argument used in proving (10) for each "single constraint" problem, we see that each pair $\langle \tilde{\boldsymbol{p}}^{(k)}, \tilde{\alpha}_k \rangle$ found solving problem (13) is also a solution to corresponding "single constraint" problem in (12), so the previously proven result establishes the present one.

□

Proof of Lemma 7. By Lemma 2(d), $\tilde{\boldsymbol{p}} \in \partial\mathcal{H}(S_{\boldsymbol{P}}(\bar{\boldsymbol{p}}, R), \bar{\boldsymbol{p}}, \tilde{\alpha})$ which is a hyper-sphere with center $\bar{\boldsymbol{p}}$ and radius $\tilde{\alpha}R$. Thus, $\rho_{\mathcal{S}} \triangleq \|\tilde{\boldsymbol{p}} - \bar{\boldsymbol{p}}\| = \tilde{\alpha}R$. □

Proof of Lemma 8. Immediate from Lemma 4 and $\rho_{\mathcal{S}} = \tilde{\alpha}R$ since $\rho_{\mathcal{S}} \geq R \Leftrightarrow \tilde{\alpha}R \geq R \Leftrightarrow \tilde{\alpha} \geq 1$. □

Proof of Lemma 10. This is immediate from Lemma 4, the earlier observation that $\tilde{\alpha} = Q(\tilde{\boldsymbol{p}}) = \tilde{\boldsymbol{q}}$ and the definition of $\rho_{\mathcal{R}}$ given in Equation (23). □

Proof of Lemma 11. If $\boldsymbol{d}$ is robust for $\mathcal{S}_{\boldsymbol{p}}(\bar{\boldsymbol{p}}, R_{out})$, Lemma 4 and Lemma 8 imply that $\boldsymbol{d}$ is robust for $\Delta_{\boldsymbol{p}}$ since $\Delta_{\boldsymbol{p}} \subseteq \mathcal{S}_{\boldsymbol{p}}(\bar{\boldsymbol{p}}, R_{out})$. Conversely, if $\boldsymbol{d}$ is non robust for $\mathcal{S}_{\boldsymbol{p}}(\bar{\boldsymbol{p}}, R_{in})$, $\exists \boldsymbol{p}^* \in \mathcal{S}_{\boldsymbol{p}}(\bar{\boldsymbol{p}}, R_{in})$ for which $\boldsymbol{g}(\boldsymbol{p}^*, \boldsymbol{d}) > \boldsymbol{0}$. Since $\boldsymbol{p}^* \in \Delta_{\boldsymbol{p}}$ and $\mathcal{S}_{\boldsymbol{p}}(\bar{\boldsymbol{p}}, R_{in}) \subseteq \Delta_{\boldsymbol{p}}$, $\boldsymbol{d}$ is non-robust. □

Proof of Lemma 12. If $\Delta_{\boldsymbol{p}} \subset \mathcal{M}$, the RDS corresponding to $\mathcal{M}$ is a subset of the RDS of $\Delta_{\boldsymbol{p}}$. Since the RDS for $\mathcal{M}$ set $\mathcal{M}$ is non-empty, so it is the one for $\Delta_{\boldsymbol{p}}$. The implication of an empty RDS results from using Lemma 8 or Lemma 10 and using $\mathcal{M} \subset \Delta_{\boldsymbol{p}}$. □

References

[1]Crespo, L. G. and Kenny, S. P., "Reliability-based control design for uncertain systems," *AIAA Journal of Guidance, Control, and Dynamics*, Vol. 28, No. 4, 2005.

[2]Kall, P. and Wallace, S., *Stochastic Programming*, Wiley, New York, 1994.

[3]Romero, V. and Chen, C.-H., "Seminal concepts for a new approach to continuous variable optimization under uncertainty: Probabilistic Ordinal Optimization," *AIAA Multidisciplinary Analysis and Optimization Conference, Albany, New York*, Vol. 6, AIAA 2004-4597, pp. 1–12.

[4]Ermoliev, Y., "Stochastic quasigradient methods and their applications to systems optimization," *Stochastics*, Vol. 9, No. 1, 1983, pp. 1–36.

[5]Darligton, J., Pantelides, C., Rustem, B., and Tanyi, B., "An algorithm for constrained nonlinear optimization under uncertainty," *Automatica*, Vol. 35, 1999, pp. 217–228.

[6]Mulvey, J. N., Vanderbrei, R. J., and Zenios, S. A., "Robust optimization of large scale systems," *Operations Research*, Vol. 2, No. 43, 1995, pp. 264–280.

[7]Gustafson, S. A., *Semi-infinite programming and applications*, Springer, Berlin, 1981.

[8]Howe, M. A., Rustem, B., and Selby, M. J. P., "Multi-period minimax hedging strategies," *European Journal of Operations Research*, Vol. 1, No. 93, 1996, pp. 185–204.

[9]Rustem, B. and Nguyen, Q., "An algorithm for the inequality constrained minimax problem," *SIAM Journal of Optimization*, Vol. 8, No. 1, 1998, pp. 265–283.

[10]Tenne, D. and Singh, T., "Efficient Minimax Control Design for Prescribed Parameter Uncertainty," *AIAA Journal of Guidance, Control and Dynamics*, Vol. 27, No. 6, 2004, pp. 1009–1016.

[11]Weisstein, E. W., "Homothetic," From MathWorld – A Wolfram Web Resource. `http://mathworld.wolfram.com/Homothetic.html`.

[12]Humphreys, A., "Star Convex," From MathWorld – A Wolfram Web Resource, created by Eric W. Weisstein. `http://mathworld.wolfram.com/StarConvex.html`.

[13]Rackwitz, R., "Reliability analysis, a review and some perspectives," *Structural Safety*, Vol. 23, 2001, pp. 365–395.

[14]Royset, J., Kiureghian, A. D., and Polak, E., "Reliability-based optimal structural design by the decoupling approach," *Reliability Engineering and System Safety*, Vol. 73, 2001, pp. 213–221.